Research article

How many sirtuin genes are out there? evolution of sirtuin genes in vertebrates with a description of a new family member*

Juan C. Opazo[1,2,3], Michael W. Vandewege[4], Federico G. Hoffmann[5,6], Kattina Zavala[2], Catalina Meléndez[7], Charlotte Luchsinger[8], Viviana A. Cavieres[7], Luis Vargas-Chacoff[1,9,10,11], Francisco J. Morera[1,12], Patricia V. Burgos[7,13,14], Cheril Tapia-Rojas[7,13], Gonzalo A. Mardones[1,8,15]

[1]Integrative Biology Group, Universidad Austral de Chile, Valdivia, Chile.
[2]Instituto de Ciencias Ambientales y Evolutivas, Facultad de Ciencias, Universidad Austral de Chile, Valdivia, Chile.
[3]Millennium Nucleus of Ion Channel-Associated Diseases (MiNICAD), Valdivia, Chile.
[4]College of Veterinary Medicine, North Carolina State University, Raleigh, NC, 27607, USA
[5]Department of Biochemistry, Molecular Biology, Entomology, and Plant Pathology, Mississippi State University, Starkville, Mississippi, USA.
[6]Institute for Genomics, Biocomputing and Biotechnology, Mississippi State University, Starkville, Mississippi, USA.
[7]Centro de Biología Celular y Biomedicina (CEBICEM), Facultad de Medicina y Ciencia, Universidad San Sebastián, Santiago, Chile.
[8]Department of Physiology, School of Medicine, Universidad Austral de Chile, Valdivia, Chile.
[9]Instituto de Ciencias Marinas y Limnológicas, Universidad Austral de Chile, Valdivia, Chile.
[10]Centro Fondap de Investigación de Altas Latitudes (IDEAL), Universidad Austral de Chile, Valdivia, Chile.
[11]Millennium Institute Biodiversity of Antarctic and Subantarctic Ecosystems, BASE, Universidad Austral de Chile, Valdivia, Chile.
[12]Applied Biochemistry Laboratory, Facultad de Ciencias Veterinarias, Instituto de Farmacología y Morfofisiología, Universidad Austral de Chile, Valdivia, Chile.
[13]Centro Ciencia & Vida, Fundación Ciencia & Vida, Santiago, Chile.
[14]Centro de Envejecimiento y Regeneración (CARE-UC), Facultad de Ciencias Biológicas, Pontificia Universidad Católica, Santiago, Chile.
[15]Center for Interdisciplinary Studies of the Nervous System (CISNe), Universidad Austral de Chile, Valdivia, Chile.

* This article is dedicated to the memory of Francisco Bozinovic and Andrés Rivera-Dictter

Corresponding authors:
Juan C. Opazo, jopazo@gmail.com
Gonzalo A. Mardones, gonzalo.mardones@uach.cl

Abstract

Studying the evolutionary history of gene families is a challenging and exciting task with a wide range of implications. In addition to exploring fundamental questions about the origin and evolution of genes, disentangling their evolution is also critical to those who do functional/structural studies to allow a deeper and more precise interpretation of their results in an evolutionary context. The sirtuin gene family is a group of genes that are involved in a variety of biological functions mostly related to aging. Their duplicative history is an open question, as well as the definition of the repertoire of sirtuin genes among vertebrates. Our results show a well-resolved phylogeny that represents an improvement in our understanding of the duplicative history of the sirtuin gene family. We identified a new sirtuin gene family member (*SIRT3.2*) that was apparently lost in the last common ancestor of amniotes but retained in all other groups of jawed vertebrates. According to our experimental analyses, elephant shark SIRT3.2 protein is located in mitochondria, the overexpression of which leads to an increase in cellular levels of ATP. Moreover, *in vitro* analysis demonstrated it has deacetylase activity being modulated in a similar way to mammalian SIRT3. Our results indicate that there are at least eight sirtuin paralogs among vertebrates and that all of them can be traced back to the last common ancestor of the group that existed between 676 and 615 millions of years ago.

Keywords: aging, deacetylase, gene family evolution, gene duplication, mitochondria, SIRT.

Introduction

The availability of whole-genome sequences in species of all main groups of vertebrates represents an opportunity to unravel the evolution of gene families. The number of genomes and their phylogenetic representativeness in the vertebrate tree of life allows performing robust inferences regarding how gene family members are related to each other and their modes of evolution (Nei and Rooney 2005). The available genomes also open an opportunity to discover new gene lineages that are not currently described maybe because they are not present in model species and/or to the absence of appropriate evolutionary analyses (Wichmann et al. 2016; Céspedes et al. 2017; Himmel et al. 2020). Gene copy number variation could be seen as a natural experiment (Albertson et al. 2009) that could help understand the evolutionary fate of duplicated genes, as individuals with different repertoires can, in principle, fulfill the biological functions with a different combination of paralogs (Gitelman 2007).

The sirtuin gene family, class III of histone deacetylase enzymes (HDACs), is a group of genes that in deuterostomes (the group that includes chordates, echinoderms, and hemichordates), is composed of seven paralogs (*SIRT1-7*) grouped into four classes (Fig. 1)(Frye 2000; Frye 2006). Sirtuin genes are involved in a variety of biological functions mostly related to aging, metabolic regulation, stress response, cell cycle among others (Fig. 1) (Michan and Sinclair 2007; Greiss and Gartner 2009; Haigis and Sinclair 2010; Zhao et al. 2019; Zhang et al. 2020). All sirtuin genes have a conserved catalytic domain and variable carboxy- and amino terminal domains. Sirtuins commonly possess NAD-dependent acyl-lysine deacylase activity (most commonly deacetylase activity), while some sirtuins may have, in addition to deacetylase activity, other enzymatic activities like ADP-ribosyltransferase, desuccinylase and demalonylase (Fig. 1). Further, they are located in different subcellular compartments and associated to different biological functions (Fig. 1).

The evolution of the sirtuin genes is an active area of investigation. There are multiple phylogenetic hypotheses describing evolutionary relationships among the orthologs and paralogs in the sirtuin gene family (Frye 2000; North and Verdin 2004; Frye 2006; Greiss and Gartner 2009; Pereira et al. 2011; Slade et al. 2011; Vassilopoulos et al. 2011; Costantini et al. 2013; Scholte et al. 2017; Simó-Mirabet et al. 2017; Yang et

al. 2017; Rajabi et al. 2018; Kabiljo et al. 2019; Zhao et al. 2019; Gold & Sinclair 2022). Differences in the taxonomic sampling, number of orthologs and/or paralogs included, and the inclusion of outgroups are likely contributors to this variation. Additionally, studies that are focused on resolving evolutionary relationships are scarce, and in fact, most phylogenetic analyses for sirtuin genes are part of studies where the sirtuin duplicative history is a secondary goal. Additionally, and probably for similar reasons, there are no systematic efforts to characterize the full complement of sirtuin genes among vertebrates. Thus, unraveling the evolutionary history of sirtuin genes represents a challenging and exciting task with a wide range of implications. Because of their role in the aging process, these genes are of great interest. In addition to exploring fundamental questions about the origin and evolution of sirtuin genes, disentangling their evolution is also critical to understanding the diversification of functional and structural phenotypes present in the sirtuin gene family.

This study aims to take advantage of the genomic data available in public databases to advance our understanding of the diversity of vertebrate sirtuin genes and to infer its duplicative history. We also aim to characterize the subcellular localization, enzymatic activity, and mitochondrial activity of the *SIRT3.2* gene (a SIRT3-paralog gene) in the elephant shark (*Callorhinchus milii*) as a representative species. Our phylogenetic tree is in general well resolved, recovering vertebrate sirtuin genes into three clades: 1) SIRT4, SIRT5, 2) SIRT6 and SIRT7, and 3) SIRT1, SIRT2, SIRT3, and SIRT3.2. The sirtuin family member SIRT3.2 is found in jawed fish and amphibians, but is absent in earlier branching deuterostomes (e.g. cephalochordates, urochordates, echinoderms and hemichordates), is absent in cyclostomes (jawless fish), and is absent in amniotes (the group that includes mammals, birds, and reptiles). Based on how sirtuin genes are related to each other and the information which is already known for the other sirtuin family members, particularly SIRT3, we can predict that SIRT3.2 belongs to the class I, has a deacetylase activity, and is mainly located in mitochondria. Our experimental analyses confirmed our evolutionary guided inferences.

Results and Discussion

Vertebrate sirtuin paralogs are recovered into three main clades

We recovered the monophyly of all sirtuin family members with strong support (Fig. 2). The diversity of sirtuin genes was arranged into three main clades (Fig. 2). The first clade contains the SIRT4 and SIRT5 paralogs, the second clade contains the SIRT6 and SIRT7 paralogs, and the third clade includes the SIRT1, SIRT2, SIRT3 and SIRT3.2 gene lineages (Fig. 2). A diversity of phylogenetic arrangements for sirtuin genes have been proposed in the past (Frye 2000; Frye 2006; Greiss and Gartner 2009; Slade et al. 2011; Vassilopoulos et al. 2011; Costantini et al. 2013; Scholte et al. 2017; Simó-Mirabet et al. 2017; Yang et al. 2017; Rajabi et al. 2018; Kabiljo et al. 2019; Zhao et al. 2019; Gold & Sinclair 2022), and our results largely support the relationships proposed by Frye (2006).

In the first clade we recovered the sister group relationships between SIRT4 and SIRT5 with strong support (Fig. 2). Evolutionary relationships between these two family members are still a matter of debate, as a variety of phylogenetic positions have been suggested for these paralogs (Slade et al. 2011; Vassilopoulos et al. 2011; Costantini et al. 2013; Yang et al. 2017; Rajabi et al. 2018; Gold & Sinclair 2022), and only in a fraction of the studies their sister group relationship is supported (Frye 2000; North and Verdin 2004; Frye 2006; Greiss and Gartner 2009; Hirschey 2011; Scholte et al. 2017; Simó-Mirabet et al. 2017; Kabiljo et al. 2019; Zhao et al. 2019). In the second clade, we recovered SIRT6 sister to the clade containing SIRT7 sequences with strong support (Fig. 2). The sister group relationship between SIRT6 and SIRT7 has been recovered in all examined studies (Frye 2000; North and Verdin 2004; Greiss and Gartner 2009; Hirschey 2011; Slade et al. 2011; Vassilopoulos et al. 2011; Costantini et al. 2013; Scholte et al. 2017; Simó-Mirabet et al. 2017; Yang et al. 2017; Rajabi et al. 2018; Kabiljo et al. 2019; Zhao et al. 2019; Gold & Sinclair 2022), suggesting there is robust support for the sister relationship between these sirtuin family members. In the third clade, there is a broad consensus in the literature that SIRT2 shares a common ancestor more recently in time with SIRT3 than with any other sirtuin paralog, and that the clade containing SIRT1 sequences is sister to the SIRT2/SIRT3 clade (Frye 2000; North and Verdin 2004; Frye 2006; Greiss and Gartner 2009; Hirschey 2011; Slade et al. 2011;

160 Vassilopoulos et al. 2011; Costantini et al. 2013; Scholte et al. 2017; Simó-Mirabet et al.
161 2017; Yang et al. 2017; Rajabi et al. 2018; Zhao et al. 2019). We recovered the same
162 evolutionary relationships with strong support (Fig. 2). The sister-group relationship
163 between the SIRT6/SIRT7 and SIRT2/SIRT3/SIRT3.2/SIRT1 received moderate support
164 (Fig. 2). The sister-group relationships among the three main sirtuin clades is something
165 that has been difficult to resolve (Simó-Mirabet et al. 2017; Zhao et al. 2019), as it
166 appears divergences were close in time, as evidence by the short length of the
167 corresponding branch (Fig. 2).
168 In summary, we present a phylogenetic analysis based on a taxonomic sampling that
169 included representative species from all main groups of vertebrates for all sirtuin family
170 members. Our phylogenetic tree is in general well resolved (Fig. 2), representing an
171 advance in our understanding of the duplicative history of the sirtuin gene family. In
172 comparison to the phylogenetic trees currently available in the literature only one study
173 shows the same topology as our study (Frye 2006).
174

175 Identification of a new sirtuin gene family member, *SIRT3.2*

176 In our analyses, we identified a new sirtuin family member (Fig. 2 and 3), *SIRT3.2*, which
177 is present in a fraction of the vertebrate tree of life (Fig. 4) that was recovered sister to
178 the *SIRT3* clade with strong support (Fig. 2 and 3). Synteny conservation provides further
179 support to the monophyly of the *SIRT3.2* gene lineage in gnathostomes (Fig. 5a), as
180 genes found at the 5` side (*POLR3B*, *RFX4* and *RIC8B*) and 3` side (*TMEM263*,
181 *MTERF2*, and *CRY1*) of the *SIRT3.2* gene are well conserved (Fig. 5a). Synteny is also
182 conserved in species in which the *SIRT3.2* gene was lost (Fig. 5a). Among vertebrates,
183 we found orthologs of the *SIRT3.2* gene in representative species of cartilaginous fish,
184 bony fish, coelacanth, lungfish and amphibians (Fig. 4). A comparison of the genomic
185 region of the tropical clawed frog (*Xenopus tropicalis*), which possesses the *SIRT3.2*
186 gene, with the corresponding region in the human (*Homo sapiens*), opossum
187 (*Monodelphis domestica*), chicken (*Gallus gallus*), gharial (*Gavialis gangeticus*), red-
188 eared slider (*Trachemys scripta*) and green anole (*Anolis carolinensis*) strongly suggests
189 that the *SIRT3.2* gene is not present in the vertebrate lineages that these species
190 represent (Fig. 5b). Interestingly, traces of the SIRT3.2 gene are present in the red-eared

191 slider (*Trachemys scripta*) genome (Fig. 5b). The absence of the *SIRT3.2* gene in
192 mammals, birds and reptiles indicates that it was probably lost in the common ancestor
193 of the group, between 352 and 312 millions of years ago (Kumar et al. 2017). In the case
194 of cyclostomes, we found in the sea lamprey (*Petromyzon marinus*) a chromosomal
195 region (Chr3) that possess *TMEM263* and *POLR3B* separated by 44 base pairs,
196 suggesting that all the genes that should be in between (*RFX4*, *RIC8B*, *SIRT3.2*) were
197 lost in cyclostomes. Alternatively, it is possible that *SIRT3.2*, and all the other genes are
198 present in cyclostome genomes, but not in the current genome assembly. In the past,
199 Pereira et al. (2011), with a limited taxonomic sampling, identified a clade sister to a group
200 containing *SIRT3* sequences. This gene lineage included sequences from three species
201 with an evolutionary history of whole-genome duplications, two teleost fish (zebrafish,
202 *Danio rerio*, and green spotted puffer, *Tetraodon nigroviridis*), and one amphibian (African
203 clawed frog, *Xenopus laevis*), complicating the definition of their duplicative history. Thus,
204 our results, including a balanced taxonomic sampling of all main vertebrate groups and
205 appropriate phylogenetic searches, define the existence of the *SIRT3.2* gene lineage and
206 its phyletic distribution. In agreement with Gold and Sinclair (2022), more extensive
207 sampling in deuterostomes, now including in addition to vertebrates, urochordates,
208 cephalochordates, echinoderms, and hemichordates, confirms that the duplication event
209 that gave rise to SIRT3 and SIRT3.2 occurred in the last common ancestor of vertebrates
210 (Supplementary figures 1 and 2).

211 The lack of the *SIRT3.2* gene can be interpreted in different ways. We can think
212 that the loss of *SIRT3.2* could have no physiological impact if the functional role of the
213 lost gene is assumed by other family members, consistent with the idea that gene families
214 possess functional redundancy (Ohno 1985; Félix and Barkoulas 2015; Albalat and
215 Cañestro 2016). Alternatively, we can also think of gene loss as a source of adaptive
216 evolution (Olson 1999; Nery et al. 2014; Albalat and Cañestro 2016; Helsen et al. 2020).
217 The description of new gene lineages is not uncommon in the literature (Wichmann et al.
218 2016; Himmel et al. 2020; Opazo et al. 2021; Gold & Sinclair 2022), and it could be mainly
219 attributed to the presence in non-model species and/or the absence of proper
220 evolutionary analyses. The existence of species with different gene repertoires is an

221 opportunity to better understand the evolutionary fate of duplicated genes (Lynch and
222 Conery 2000) and the biological functions associated with a group of genes.

223 An amino acid alignment of the SIRT3.2 and SIRT3 sequences shows that the
224 catalytic domain of SIRT3.2 is well conserved, where six amino acid positions were
225 identified as diagnostic characters (Fig. 6). The amino acid divergence of the SIRT3.2
226 catalytic domain varies from 32.2% (spotted gar vs coelacanth) to 33.6% (spotted gar vs
227 elephant shark). The same comparisons for the SIRT3 catalytic domain show slightly
228 lower amino acid divergence values, between 24.8% (spotted gar vs coelacanth) and
229 31.0% (coelacanth vs elephant shark). As expected, the interparalog distance (SIRT3 vs
230 SIRT3.2) of the catalytic domains shows higher divergence values, ranging from 40.7%
231 (spotted gar SIRT3 vs spotted gar SIRT3.2) and 43.6% (elephant shark SIRT3 vs
232 elephant shark SIRT3.2). Although nothing is known about the protein encoded by the
233 SIRT3.2 gene, based on how sirtuin genes are evolutionarily related and the information
234 already known for the other family members (Fig. 1), we can speculate that SIRT3.2
235 belongs to the class I, is mainly located on the mitochondria/nucleus, and has deacetylase
236 activity. From a functional perspective it should perform functions similar to what has been
237 described for SIRT3 (Fig. 1) (Brown et al. 2013; McDonnell et al. 2015; Zhang et al. 2020).
238 It is important to highlight that the inferences regarding a newly discovered gene are better
239 performed if they are phylogenetically guided.

240 Expression pattern of sirtuin gene family members

241 Our next step in characterizing the *SIRT3.2* gene was to investigate whether it is
242 transcribed and if it was, to characterize the transcription pattern. To do this, we mapped
243 RNASeq reads to reference gene sequences of representative species of vertebrates and
244 examined transcript abundance. In agreement with the transcription pattern reported for
245 sirtuin genes (Stelzer et al. 2016; Kabiljo et al. 2019), our results show that although they
246 exhibited wide variance in tissue expression, sirtuin genes are expressed in almost all
247 tissues, including the novel *SIRT3.2* gene lineage (Fig. 7). In the case of the tropical
248 clawed frog, the *SIRT3.2* gene is transcribed at a similar level in all tissues, other than
249 the ovary where high transcription levels were estimated (Fig. 7). Coincident with the
250 pattern observed in the tropical clawed frog, the elephant shark *SIRT3.2* gene is mostly
251 transcribed in the ovary (Fig. 7). These results should be taken with caution given the lack

252 of biological replicates, at least within species. In the case of the zebrafish, although our
253 transcription level estimations did not follow the trend previously mentioned, an extensive
254 study examining the expression of all sirtuin genes in zebrafish showed that the *SIRT3.2*
255 gene in this species is mainly expressed in the ovary (Pereira et al. 2011). Thus, in
256 addition to showing that the *SIRT3.2* gene is transcribed, our analyses allow us to suggest
257 that this gene could be involved in biological processes associated with reproduction. This
258 observation agrees with the literature as for SIRT3 there are many studies in which its
259 functions related to reproduction have been reported (Zhao et al. 2016; Tatone et al. 2018;
260 Vazquez et al. 2020; Di Emidio et al. 2021).
261

262 Elephant shark SIRT3.2 protein localizes to mitochondria

263 To further explore the structural relationship between SIRT3 and SIRT3.2 proteins, we
264 performed an unbiased protein structure modeling of SIRT3.2 proteins from elephant
265 shark (*Callorhinchus milii*), spotted gar (*Lepisosteus oculatus*), salmon (*Salmo salar*) and
266 coelacanth (*Latimeria chalumnae*). Models of SIRT3.2 proteins were generated by the
267 SWISS-MODEL workspace that used as template crystal structure models of human
268 SIRT3: 4bvh.1.A for elephant shark, 5z94.1.A for spotted gar, 5d7n.3.A for salmon and
269 5bwo.1.B for coelacanth (data not shown). All models generated comprise only the central
270 portion of the SIRT3.2 proteins where the catalytic and its regulatory regions are expected
271 to be: amino acids G95 to Q365 for elephant shark, L115 to V388 for spotted gar, P114
272 to G387 for salmon, and K113 to P386 for coelacanth. The overall root mean square
273 deviation for 272 superimposable Cα coordinates for the models of human SIRT3 (pdb:
274 4bvh.1.A; amino acids G121 to G392) and elephant shark SIRT3.2 (amino acids G95 to
275 Q365) is 0.101 Å (Fig. 8a), suggesting extensive structural match. Some SIRT proteins,
276 such as SIRT1, SIRT2 and SIRT3, possess evolutionarily conserved, distinct cellular
277 localizations and functions, as evidenced by their analysis in several model species that
278 include Drosophila melanogaster, Mus musculus and Homo sapiens (McBurney et al.
279 2003; Blander and Guarente 2004; North and Verdin 2004; Michishita et al. 2005; Haigis
280 et al. 2006) (Fig. 1). Some sirtuins localize in more than one compartment, like SIRT1

281 and SIRT2 that localize to the nucleus and cytosol, and SIRT3 that localizes mainly to the
282 mitochondrial matrix, but with a small fraction localizing to the nucleus (Scher et al. 2007).
283 In contrast, SIRT4 and SIRT5 localize only to mitochondria, and SIRT6 and SIRT7
284 localize only to the nucleus. The sequence and structural comparison between SIRT3.2
285 and SIRT3 proteins, as well as subcellular localization prediction by LocTree3 (Goldberg
286 et al. 2014), suggest that the localization of SIRT3.2 proteins is also in the mitochondria.
287 To determine the subcellular localization of SIRT3.2 proteins, we chose to analyze
288 SIRT3.2 from elephant shark. To this end, we expressed in human cultured cells full-
289 length elephant shark SIRT3.2 tagged with three copies of the c-Myc epitope at the C-
290 terminus (SIRT3.2-3myc). To obtain biochemical evidence of the expression of this
291 protein, we performed immunoblot analysis with monoclonal antibody 9E10 against the
292 c-Myc epitope, which showed the detection of an expected 48.3 kDa protein in all cell
293 lines analyzed (Fig. 8b). Fluorescence microscopy analysis of human H4 neuroglioma
294 cells expressing SIRT3.2-3myc showed decoration by the anti-c-Myc antibody of
295 structures highly reminiscent of mitochondria, in addition to a faint fluorescent signal in
296 the rest of the cytoplasm (Fig. 8c, d). Mitochondria localization of SIRT3.2-3myc was
297 confirmed by co-localization with the fluorescent signal of MitoTracker Orange (Pearson's
298 correlation coefficient [r] = 0.94 ± 0.02; *n* = 20; Fig. 8c and Supplementary Fig. 3a).
299 Importantly, SIRT3.2-3myc showed no localization in any other major compartment, as
300 shown by lack of localization in the nucleus (detected with the nuclear stain DAPI; r = 0.21
301 ± 0.03; *n* = 20; Fig. 8c, d and Supplementary Fig. 3b), the Golgi apparatus (detected with
302 antibody against Trans-Golgi network integral membrane protein 2 (TGN46)
303 (Ponnambalam et al. 1996) (r = 0.34 ± 0.09; *n* = 20; Fig. 8c, d and Supplementary Fig.
304 3c), or the endoplasmic reticulum (detected with antibody against Cytoskeleton-
305 associated protein 4 (P63) (Schweizer et al. 1993) (r = 0.47 ± 0.15; *n* = 20; Fig. 8d and
306 Supplementary Fig. 3d). The same pattern of expression of SIRT3.2-3myc was obtained
307 using other human cell lines, such as HeLa or MDA-MB-231 cells (data not shown).
308 Altogether, these results indicate that SIRT3.2 proteins are targeted to the mitochondria.
309

310 ## Elephant shark SIRT3.2 protein has deacetylase activity

311 Reversible lysine acetylation is one of the most common post-translational modifications
312 on proteins that regulate a variety of physiological processes including gene expression,
313 enzymatic activity, protein-protein interactions, and subcellular localization (Glozak et al.
314 2005). Sirtuin proteins share a catalytic core domain (North and Verdin 2004) that have
315 NAD^+-dependent deacetylase activity (Shahgaldi and Kahmini 2021). After translocation
316 into the mitochondrial matrix, human SIRT3 is inactive, but after proteolytic processing of
317 its N-terminus signal peptide it becomes active as deacetylase (Onyango et al. 2002;
318 Schwer et al. 2002). Similar to human SIRT3, secondary structure prediction of
319 representative SIRT3.2 proteins indicates that the first ~100 N-terminal amino acids are
320 in a disordered domain (data not shown). Therefore, to determine if SIRT3.2 proteins also
321 exhibit deacetylase activity, we produced in bacteria N-terminal truncated elephant shark
322 SIRT3.2 protein (amino acids 95-372; **Δ**NT-SIRT3.2). To analyze the enzymatic activity
323 of purified **Δ**NT-SIRT3.2, we used a commercial fluorometric deacetylation activity assay
324 that contains an acetylated substrate peptide for recombinant human SIRT3 (Abcam). An
325 initial analysis of activity at 37ºC showed that **Δ**NT-SIRT3.2 possesses a deacetylase
326 activity that is similar to that of human SIRT3, being also NAD^+-dependent (Fig. 9a, e, f).
327 Because the enzymatic activity of elephant shark SIRT3.2 could be influenced by the
328 environmental conditions, we next evaluated the optimal temperature of **Δ**NT-SIRT3.2
329 compared to that of human SIRT3. As expected, the optimal temperature of the human
330 SIRT3 was ~37ºC (Fig. 9b). In contrast, **Δ**NT-SIRT3.2 exhibited an optimal temperature
331 at ~24ºC (Fig. 9b). The optimal temperature value for the SIRT3.2 deacetylase activity of
332 the elephant shark could represent an evolutionary adjustment to the temperature regime
333 of the habitat in which this species lives, as it has been demonstrated for other enzymes
334 in other species (McCormick 1993; Somero 2004; Bilyk et al. 2021; Saravia et al. 2021).
335 Thus, all subsequent enzymatic activity analyses for **Δ**NT-SIRT3.2 were performed at
336 24ºC. The apparent specific activity of **Δ**NT-SIRT3.2 was 260.7 ± 9.9 fluorescence units
337 (FU) min^{-1} mg^{-1}, which was significantly lower than that of SIRT3 that was 1143.3 ± 46.3
338 FU min^{-1} mg^{-1}. Apparent K_m of **Δ**NT-SIRT3.2 and SIRT3 were 5.7 and 5.5, respectively,
339 which resulted not significantly different (Fig. 9c, d). In contrast, apparent V_{max} of **Δ**NT-
340 SIRT3.2 was 0.322 FU sec^{-1}, which was significantly different to that of SIRT3 that was
341 3.908 FU sec^{-1} (Fig. 9c, d). We next compared the effect of the sirtuin inhibitors

342 nicotinamide (NAM) (Sauve and Schramm 2003) and quercetin (QUE) (You et al. 2019)
343 on the activities of SIRT3 and ΔNT-SIRT3.2. As expected, SIRT3 activity was significantly
344 inhibited by NAM and QUE (Fig. 9e). We also found a significant inhibitory effect of both
345 NAM and QUE on the activity of ΔNT-SIRT3.2 (Fig. 9f). We also compared the effect of
346 the polyphenolic antioxidant resveratrol (REV), which is an activator of sirtuins (Wood et
347 al. 2004). As expected, we found a significant concentration-dependent activation of
348 SIRT3 deacetylase activity up to a 1.6 ± 0.1-fold increase in the presence of 100 μM REV
349 (Fig. 9e). Strikingly, we found a much more potent concentration dependent activation
350 effect of REV on ΔNT-SIRT3.2, showing up to a 11.1 ± 0.6 fold increase in the presence
351 of 100 μM REV (Fig. 9f). However, because the specific activity of ΔNT-SIRT3.2 was
352 ~23% that of SIRT3 in the assay conditions, the activation of ΔNT-SIRT3.2 by REV in fact
353 represents a value only ~1.6 fold higher compared to the activation of SIRT3 by REV.
354 Because different sirtuins have activity on different proteins, as well as remove with
355 different specificity a variety of acyl groups other than the acetyl (Fig. 1) (Anderson et al.
356 2014), the modulation of ΔNT-SIRT3.2 activity by REV suggests that it has distinct
357 functional substrates. Together, these results demonstrate that elephant shark ΔNT-
358 SIRT3.2 has deacetylase activity and indicate that the activity of SIRT3.2 proteins is
359 modulated in a similar manner to that of mammalian sirtuins.
360

361 ## Elephant shark SIRT3.2 protein increases ATP cellular content

362 Considering that SIRT3 plays an important role in maintaining basal ATP levels by
363 deacetylation of mitochondrial proteins involved in electron transport chain (ETC), the
364 tricarboxylic acid cycle, and fatty-acid oxidation (Hirschey et al. 2010), we investigated
365 the impact of transient SIRT3.2-3myc expression on ATP cellular content in H4 and HeLa
366 cells (Fig. 10a). Similar to the well-known effect of mammalian SIRT3, SIRT3.2-3myc
367 expression increased ATP cellular content, suggesting that it shares with SIRT3 the ability
368 to enhance the activity of the mitochondrial ETC. Because an enhancement in the activity
369 of ETC can cause an increase in reactive oxygen species (ROS), we also evaluated the
370 levels of ROS in cells expressing SIRT3.2-3myc (Fig. 10b). We found similar ROS levels
371 in cells expressing SIRT3.2-3myc and untransfected cells (Fig. 10b). This finding
372 suggests that SIRT3.2 proteins share the mammalian SIRT3 characteristic of protection

373 against oxidative damage (Bause and Haigis 2013), likely by deacetylation of enzymes
374 involved in ROS clearance to protect mitochondrial membranes from oxidative stress
375 (Tseng et al. 2013). A candidate that could be activated by the deacetylation activity of
376 SIRT3.2 proteins is SOD2 that in human cells reduces cellular ROS content promoting
377 oxidative stress resistance (Qiu et al. 2010; Tao et al. 2010). Alternatively, SIRT3.2
378 proteins could activate the last complex of the ETC by deacetylation, enhancing ATP-
379 synthase activity without affecting ROS production, similar to the effect that SIRT3 has in
380 response to exercise-induced stress (Vassilopoulos et al. 2014). Together, our results
381 show that the SIRT3.2 protein is a new sirtuin family member with deacetylase activity
382 that could have important roles in the homeostasis of oxidative species and mitochondrial
383 metabolism.
384

385 ## Conclusions

386 We performed an evolutionary analysis of the sirtuin gene family in vertebrates. In
387 addition to describing the duplicative history of sirtuins, our phylogenetic analyses
388 revealed the presence of a new gene family member, *SIRT3.2*. This new vertebrate gene
389 lineage is present in all vertebrates other than mammals, birds, and reptiles. Furthermore,
390 our transcriptomic analyses show that *SIRT3.2* is transcribed in almost all examined
391 tissues, showing a tendency to be more expressed in the ovary, suggesting biological
392 functions related to reproduction. According to our analyses, SIRT3.2 localized in the
393 mitochondria, had deacetylase activity and increased the ATP cellular content. The
394 finding of a new sirtuin gene lineage highlights the need for more detailed assessments
395 of orthology with a broader taxonomic sampling to better define the membership
396 composition of gene families (Glover et al. 2019). In the literature, there are examples in
397 which more comprehensive analyses provide a better description of gene families,
398 including previously unknown family members (Castro et al. 2012; Wichmann et al. 2016;
399 Céspedes et al. 2017; Ramos-Vicente et al. 2018; Opazo, Kuraku, et al. 2019; Opazo,
400 Hoffmann, et al. 2019). The availability of species with different gene repertoires could be
401 seen as a natural experiment (Albertson et al. 2009) that helps us understand the
402 evolutionary fate of duplicated genes, as they can fulfill the biological functions associated
403 with the gene family but with a different combination of paralogs.

Methods

Protein sequences and phylogenetic analyses

We retrieved sirtuin amino acid sequences in representative species of all main groups of vertebrates. Our sampling included mammals, birds, reptiles, amphibians, lungfish, coelacanth, bony fish, cartilaginous fish, and cyclostomes (Supplementary Table S1). Sequences were obtained from the Orthologous MAtrix project (OMA), December 2021 release (Altenhoff et al. 2021)last accessed on April 8th, 2022). In addition, we complemented our sampling by retrieving sequences from vertebrate groups that were not present or poorly represented in the Orthologous MAtrix project (e.g., crocodiles) from the National Center for Biotechnology Information (NCBI) (Sharma et al. 2019) using the program blast (tblastn) with default parameters (Altschul et al. 1990) Supplementary Table S1). Protein sequences were aligned using the software MAFFT v.7 (Katoh and Standley 2013), allowing the program to choose the alignment strategy (FFT-NS-i, alignment length 2490 amino acids). To select the best-fitting model of molecular evolution we used the proposed model tool in the program IQ-Tree v1.6.12 (Kalyaanamoorthy et al. 2017), which selected JTT+F+I+G4. We used a maximum-likelihood approach to obtain the best tree using the program IQ-Tree v1.6.12 (Trifinopoulos et al. 2016). We carried out 20 independent runs to explore the tree space changing the value of the strength of the perturbation (-pers) parameter. We conducted the following analyses:

1. Five runs modifying the strength of the perturbation parameter from 0.5 (default value) to 0.3.
2. Five runs using the default value (0.5) for the strength of the perturbation parameter.
3. Five runs modifying the strength of the perturbation parameter from 0.5 (default value) to 0.7.
4. Five runs modifying the strength of the perturbation parameter from 0.5 (default value) to 0.9.

In all cases, the number of unsuccessful iterations to stop parameter (-nstop) value was changed from 100 (default value) to 500. The tree with the highest likelihood score was

435 chosen (log-likelihood: -127052.963, -pers 0.5 and -nstop 500). Support for the nodes
436 was evaluated using two approaches: the aBayes test (Anisimova et al. 2011) and the
437 ultrafast bootstrap procedure using 1000 replicates (Hoang et al. 2018). Nicotinamide
438 Nucleotide Transhydrogenase (NNT) protein sequences, a member of the DHS-like
439 NAD/FAD-binding domain superfamily, from the human (*Homo sapiens*), mouse (*Mus*
440 *musculus*), zebrafish (*Danio rerio*) and spotted gar (*Lepisosteus oculatus*) were used as
441 outgroups.
442

443 Assessment of conserved synteny

444 We examined genes found upstream and downstream of the sirtuin genes. For
445 comparative purposes, we used the estimates of orthology and paralogy derived from the
446 Ensembl Compara database (Herrero et al. 2016); these estimates are obtained from a
447 pipeline that considers both synteny and phylogeny to generate orthology mappings.
448 These predictions were visualized using the program Genomicus v100.01 (Nguyen et al.
449 2018). Our assessments were performed in humans (*Homo sapiens*), chicken (*Gallus*
450 *gallus*), gharial (*Gavialis gangeticus*), red-eared slider (*Trachemys scripta*), green anole
451 (*Anolis carolinensis*), tropical clawed frog (*Xenopus tropicalis*), coelacanth (*Latimeria*
452 *chalumnae*), spotted gar (*Lepisosteus oculatus*), and elephant shark (*Callorhinchus milii*).
453

454 Dot-plots

455 We retrieved the chromosomal region containing the *SIRT3.2* gene of the tropical clawed
456 frog (*Xenopus tropicalis*, Ch3) including 6.7 kb up- and downstream, and the
457 corresponding syntenic region in the human (*Homo sapiens*, Chr12), opossum
458 (*Monodelphis domestica*, Chr8), chicken (*Gallus gallus*, Chr1), gharial (*Gavialis*
459 *gangeticus*, NW_017729022.1), red-eared slider (*Trachemys scripta*, Chr1), and green
460 anole (*Anolis carolinensis*, Chr5) based on the location of the flanking genes (*RIC8B* and
461 *TMEM263*). We aligned SIRT3.2 syntenic regions using Advanced PipMaker (Schwartz
462 et al. 2000).
463

464 Transcript abundance analyses

465 Sirtuin transcript abundance was measured from a representative sample of vertebrates
466 including the elephant shark (*Callorhinchus milii*), zebrafish (*Danio rerio*), tropical clawed
467 frog (*Xenopus tropicalis*), anole lizard (*Anolis carolinensis*), and human (*Homo sapiens*).
468 RNASeq libraries from brain, heart, kidney, liver, muscle, ovary, and testis from each
469 species were gathered from the NCBI Short Read Archive (SRA; (Leinonen et al. 2011).
470 Accession numbers for species and tissue specific libraries can be found in Supplemental
471 Table S2. Reference transcript sequences were collected from Ensembl v.100 (Yates et
472 al. 2020) and we removed sequences that were shorter than 100 bp. For each library
473 adapters were removed using Trimmomatic 0.38 (Bolger et al. 2014) and reads were
474 filtered for quality using the parameters HEADCROP:5, SLIDINGWINDOW:5:30, and
475 MINLEN:50. We mapped quality filtered paired-end RNAseq reads back to reference
476 sequences using Bowtie 1.2.2 (Langmead et al. 2009) and default parameters of RSEM
477 (Li and Dewey 2011). Transcripts with < 10 mapped reads across all seven tissues per
478 species were removed prior to normalization. Normalization of raw read counts for each
479 species was performed using the median of ratios (Anders and Huber 2010) method
480 implemented by the estimateSizeFactors function in DESeq2 v1.26 (Love et al. 2014).
481 Briefly, for all samples within a species, the geometric mean is calculated for the read
482 counts of each gene. Read counts are then divided by the geometric mean and the
483 median ratio is determined for each sample. Normalized read counts are calculated by
484 dividing raw read counts by the sample-specific median ratio. If multiple SIRT transcripts
485 were present, we presented the expression data from the transcript with the most mapped
486 reads.
487

488 ## Protein structure homology modeling

489 Protein structure homology modeling was performed using the SWISS-MODEL server
490 (https://swissmodel.expasy.org/) (Waterhouse et al. 2018). Structural figures were
491 prepared with PyMOL Molecular Graphics System, Version 2.0.6 Schrödinger, LLC.
492

493 ## Recombinant cDNA Constructs

494 For expression in mammalian cells, a codon-optimized mammalian expression construct
495 encoding full-length (amino acids 1-372) elephant shark (*Callorhinchus milii*) SIRT3.2

496 (Supplementary table S1), cloned in-frame into the *Eco*RI and *Sal*I sites of the pCMV-
497 3Tag-4a vector followed by vector encoding sequence of three successive Myc epitope
498 tags before a stop codon, was acquired from GenScript (Piscataway, NJ). For the
499 generation of a codon-optimized bacterial expression construct, a cDNA encoding N-
500 terminal truncated (amino acids 95-372) elephant shark SIRT3.2, cloned in-frame into the
501 *Eco*RI and *Sal*I sites of the pGEX-4T-1 vector, was also acquired from GenScript. This
502 cDNA was subsequently cloned in-frame into the *Eco*RI and *Sal*I sites of the pGST-
503 Parallel-1 vector (Sheffield et al. 1999). The nucleotide sequence of all recombinant
504 constructs was confirmed by dideoxy sequencing using the AUSTRAL-omics core facility
505 at Universidad Austral de Chile (https://australomics.cl/).
506

507 ## Cell culture, cell transfection and preparation of protein extracts

508 H4 human neuroglioma cells, HeLa human cervix adenocarcinoma cells and MDA-MB-
509 231 human mammary gland adenocarcinoma cells were obtained from the American
510 Type Culture Collection (Manassas, VA). H4 and HeLa cells were maintained in
511 Dulbecco's modified Eagle's medium (DMEM), and MDA-MB-231 in DMEM-F12
512 (ThermoFisher, Waltham, MA). For all cell lines, media were supplemented with 10%
513 heat-inactivated fetal bovine serum, 100 U/ml penicillin, 100 µg/ml streptomycin
514 (ThermoFisher), and 5 µg/ml plasmocin (InvivoGen, San Diego, CA), and cells were
515 cultured in a humidified incubator with 5% CO_2 at 37 °C. For transient transfections, cells
516 were either seeded on top of glass coverslips on 24-well plates or on 6-well plates. When
517 cells were ~60% confluent, transfections were performed with Lipofectamine 2000
518 (ThermoFisher), according to the manufacturer's instructions. Preparation of protein
519 extracts from cultured, transfected or non-transfected cells was performed using methods
520 described elsewhere (Tenorio et al. 2016).
521

522 ## Antibodies and cell reagents

523 We used the following antibodies: mouse clone 9E10 against the c-Myc epitope
524 (Covance, Princeton, NJ), mouse clone BA3R against β-ACTIN (ThermoFisher), rabbit
525 polyclonal against Cytoskeleton-associated protein 4 (P63; Merck, Germany; cat #
526 HPA001225), and sheep polyclonal against Trans-Golgi network integral membrane

527 protein 2 (TGN46; Bio-Rad Laboratories, Hercules, CA; cat # AHP500G). The following
528 fluorochrome-conjugated antibodies were from ThermoFisher: Alexa Fluor-488–
529 conjugated donkey anti mouse IgG, Alexa Fluor-594–conjugated donkey anti rabbit IgG
530 and Alexa Fluor-647-conjugated donkey anti sheep IgG. HRP-conjugated secondary
531 antibodies were from Jackson ImmunoResearch (West Grove, PA). Depending on their
532 reactivity, primary antibodies were used at a dilution 1/200 to 1/2000. HRP-conjugated
533 secondary antibodies were used at dilutions 1/5000 to 1/20000 also depending on their
534 reactivity. All Alexa Fluor-conjugated secondary antibodies were used at a dilution
535 1/1000. The fluorescent nuclear stain 4',6-diamidino-2-phenylindole (DAPI) was also from
536 ThermoFisher.
537

538 Protein Electrophoresis, Immunoblotting and Immunofluorescence 539 Microscopy

540 SDS-PAGE and immunoblotting were performed as described (Bustamante et al. 2020).
541 For fluorescence microscopy, cells grown on glass coverslips were transfected, and after
542 16-h cells were left untreated or treated for 30 min with MitoTracker™ Orange CMTMRos
543 (ThermoFisher) according to the manufacturer's instructions. After washing with
544 phosphate buffered saline (PBS) supplemented with 0.1 mM $CaCl_2$ and 1 mM $MgCl_2$
545 (PBS-CM), cells were fixed in 4% paraformaldehyde for 30 min at room temperature,
546 permeabilized with 0.2% Triton X-100 in PBS-CM for 15 min at room temperature, and
547 incubated with blocking solution (0.2% gelatin in PBS-CM) for 10 min at room
548 temperature. Cells were incubated simultaneously either with antibodies to the c-Myc
549 epitope (1/200) and to TGN46 (1/1000) or to the c-Myc epitope, to TGN46 and to P63
550 (1/600) for 30 min at 37 ºC in a humidified chamber. After washing coverslips with PBS,
551 cells were incubated as before, but with fluorochrome-conjugated antibodies, followed by
552 PBS-washing, and coverslips were mounted onto glass slides with Fluoromount-G
553 mounting medium (ThermoFisher). Fluorescence microscopy images were acquired with
554 an AxioObserver.D1 microscope equipped with a PlanApo 63x oil immersion objective
555 (NA 1.4), and an AxioCam MRm digital camera (Carl Zeiss). To quantitatively evaluate
556 colocalization of fluorescence signals, we obtained the Pearson’s correlation coefficient
557 and cytofluorograms of pairwise comparisons from images acquired under identical

558 settings, avoiding signal saturation and corrected for background, crosstalk and noise
559 signals on each set of images, using the plugin JACoP (Bolte and Cordelières 2006)
560 implemented in the software ImageJ (version 1.47h)(Schneider et al. 2012), and the
561 plugin Colocalization Finder implemented in the software ImageJ2 (version 2.3.0/1.53)
562 (Rueden et al. 2017). To prepare figures, 12-bit images were processed with ImageJ
563 software and Adobe Photoshop CS3 software (Adobe Systems, Mountain View, CA).
564

565 Expression and Purification of Recombinant N-terminal truncated elephant 566 shark SIRT3.2 protein

567 Recombinant, N-terminal truncated elephant shark SIRT3.2 (**Δ**NT-SIRT3.2; amino acids
568 95-372) tagged with an N-terminal glutathione S-transferase (GST) followed by a tobacco
569 etch virus (TEV) protease cleavage site was expressed and purified using a method
570 described previously (Ross et al. 2014), with some modifications. Briefly, expression in
571 *E. coli* B834(DE3) (Novagen, Madison, WI) was induced with 0.25 mM IPTG at 25 °C for
572 16 h. Pellets of bacteria were resuspended in homogenization buffer (50 mM Tris HCl,
573 0.5 M NaCl, 5 mM EDTA, 5 mM β-mercaptoethanol, and 2 mM phenylmethylsulfonyl
574 fluoride, pH 8.0) and lysed by sonication. The clarified supernatant was purified on
575 glutathione-Sepharose 4B (GE Healthcare). After removal of the GST moiety by TEV
576 cleavage, and sequential further passage through glutathione-Sepharose 4B and Ni-NTA
577 (QIAGEN) resins, **Δ**NT-SIRT3.2 was further purified on a Superdex 200 pg column (GE
578 Healthcare) equilibrated in storage buffer (50 mM Tris HCl, 150 mM NaCl, 1 mM DTT).
579 Aliquots of purified protein were kept at -80 ºC until use.
580

581 Deacetylation activity

582 To characterize deacetylation activity of recombinant, N-terminal truncated elephant
583 shark SIRT3.2 (**Δ**NT-SIRT3.2), we used a fluorometric SIRT3 activity assay kit (Abcam,
584 cat # ab156067; Cambridge, UK), according to the manufacturer's instructions. This
585 assay allows detection of a fluorescent signal upon deacetylation of an acetylated
586 substrate peptide for recombinant human SIRT3. The intensity of fluorescence was
587 measured on a fluorometric microplate reader (Varioskan Flash, ThermoFisher) with
588 excitation set at 350 nm and emission detection set at 450 nm. To analyze the

589 deacetylation activity of N-terminal truncated elephant shark SIRT3.2 protein, first we
590 determined its optimum temperature that resulted to be ~24 ºC. Subsequent analyses
591 were performed by comparing the activity of N-terminal truncated elephant shark SIRT3.2
592 protein at 24 ºC to that of human SIRT3, which is provided by the assay kit, at 37 ºC. K_m
593 and V_{max} were obtained by varying the concentration of the fluorogenic acetylated
594 substrate peptide provided by the assay kit. This assay was also used to determine the
595 effect of nicotinamide (NAM), quercetin (QUE) and resveratrol (REV; Sigma-Aldrich) on
596 the deacetylation activity of **Δ**NT-SIRT3.2.
597

598 ## ATP and ROS content

599 ATP levels were quantified in cell lysates using a luciferin/luciferase bioluminescence
600 assay (ATP determination kit, Molecular Probes cat # A22066, Thermo Fisher Scientific)
601 as previously described (Jara et al. 2018). Briefly, cells were lysed in HEPES buffer (125
602 mM NaCl, 25 mM NaF, 1 mM EDTA, 1 mM EGTA, 1% NP-40, 25 mM HEPES, pH 7.4)
603 supplemented with a protease inhibitor mixture (cat # 78429, Thermo Fisher Scientific)
604 and centrifuged at 12000 rpm using a refrigerated centrifuge (Eppendorf model 5424R)
605 for 15 min at 4 ºC. Proteins in the supernatant were quantified, and 10 µl of lysate were
606 used to determine ATP levels according to the kit manufacturer's instructions. The ATP
607 level in each sample was calculated using standard curves and normalized to the protein
608 concentration in each sample. ROS content was determined in cell lysates using 25 µM
609 CM-H2DCFDA (DCF; a fluorogenic indicator of ROS), as previously described (Jara et
610 al. 2018; Olesen et al. 2020). The intensity of fluorescence was measured on a
611 fluorescence plate reader (Biotek Synergy HT, Agilent, Santa Clara, CA) with excitation
612 set at 485 nm and emission detection set at 530 nm. Briefly, in a dark 96-well plate, 25
613 µg of cell lysate proteins were incubated with CM-H2DCFDA (DCF) dye with shaking for
614 5 min at room temperature, followed by determination of the fluorescence of each sample
615 that was subtracted by the fluorescence of the respective blank.
616

617 ## Statistical Analysis

618 In the case of the deacetylation, ATP content and ROS content assays, quantification
619 was performed from at least three independent experiments/measurements. Statistical

620 analysis was performed using Microsoft Excel for Mac 2011 (Microsoft Corporation).
621 When appropriate, results are represented in graphs depicting the mean ± standard
622 deviation. Statistical significance was determined by two-tailed, paired t-test. P-values >
623 0.05 or ≤ 0.05 were regarded as not statistically significant or statistically significant,
624 respectively. In the figures, P-values between 0.01 and 0.05 are indicated with one
625 asterisk, P-values between 0.001 and 0.01 are indicated with two asterisks, and P-values
626 less than 0.001 are indicated with three asterisks.
627

628 **Figure Legends**

629

630 **Figure 1.** Gene phylogeny, synteny, protein size, molecular weight, enzymatic activity,
631 subcellular localization, functions and diseases associated with sirtuin genes. Information
632 regarding the sister group relationships among sirtuin genes was obtained from this study,
633 synteny from ENSEMBL v.106 (Howe et al. 2021), protein size from Fujita and Yamashita
634 (2018)(Fujita and Yamashita 2018), molecular weight from Vassilopoulos et al.
635 (2011)(Vassilopoulos et al. 2011) while enzymatic activity, subcellular localization,
636 functions and diseases from Zhang et al. (2020)(Zhang et al. 2020). In the case of the
637 SIRT3.2 of the elephant shark, synteny information was obtained from the National
638 Center for Biotechnology Information (NCBI) (Sharma et al. 2019), protein size, molecular
639 weight, enzymatic activity and subcellular localization from this study.

640

641 **Figure 2.** Maximum likelihood tree showing sister group relationships among sirtuin
642 genes of vertebrates. Numbers on the nodes correspond to support from the aBayes and
643 ultrafast bootstrap values. Nicotinamide Nucleotide Transhydrogenase (NNT) sequences
644 from the human (*Homo sapiens*) mouse (*Mus musculus*), spotted gar (*Lepisosteus*
645 *oculatus*) and zebrafish (*Danio rerio*) were used as outgroups (not shown). The scale
646 denotes substitutions per site and colors represent vertebrate sirtuin lineages.

647

648 **Figure 3.** Maximum likelihood tree showing sister group relationships among SIRT3 and
649 SIRT3.2 genes in vertebrates. Numbers on the nodes correspond to support from the
650 aBayes and ultrafast bootstrap values. The scale denotes substitutions per site and colors
651 represent gene lineages. This tree does not represent a novel phylogenetic analysis, it is
652 the SIRT3/SIRT3.2 clade that was recovered from figure 2.

653

654 **Figure 4.** Phyletic distribution of sirtuin genes in vertebrates. The sister group
655 relationships among sirtuin genes was obtained from this study, whereas, organismal
656 phylogeny was obtained from the most updated phylogenetic hypotheses available in the
657 literature (Iwabe et al. 2005; Delsuc et al. 2006; Delsuc et al. 2008; Hara et al. 2018). The
658 colors of the circles are those used in figure 2 to define sirtuin gene lineages, whereas
659 the classes to which the different sirtuins belong are shown with shading.

660

661 **Figure 5.** a Patterns of conserved synteny in the chromosomal region that harbor SIRT3.2
662 genes in gnathostomes. Asterisks denote that the orientation of the genomic piece is from
663 3´ to 5´, gray lines represent intervening genes that do not contribute to conserved
664 synteny. b Pairwise dot-plot comparison of the genomic region of the tropical clawed frog
665 (*Xenopus tropicalis*) with the corresponding region in the human (Homo sapiens),
666 opossum (*Monodelphis domestica*), chicken (*Gallus gallus*), gharial (*Gavialis*
667 *gangeticus*), red-eared slider (*Trachemys scripta*) and green anole (*Anolis carolinensis*).
668 Light green vertical lines denote exons and regions in between are introns. Dot plots were
669 based on the complete coding region in addition to 6.7 kb of upstream and downstream
670 flanking sequence. The red circle highlights the vestiges of the fourth exon in the red-
671 eared slider (*Trachemys scripta*).The genome assembly version of the species depicted
672 in this figure is the following: Human: GRCh38.p13; Opossum: ASM229v1; Chicken:
673 GRCg6a; Gharial: GavGan_comp1; red-eared slider: CAS_Tse_1.0; Green anole:
674 AnoCar2.0v2; Tropical clawed frog: UCB_Xtro_10.0; Coelacanth: LatCha1; Spotted gar:
675 LepOcu1 and Elephant shark: Callorhinchus_milii-6.1.3.

676

677 **Figure 6.** Alignment of the catalytic domain of SIRT3 in humans (*Homo sapiens*), and
678 SIRT3 and SIRT3.2 of spotted gar (*Lepisosteus oculatus*), coelacanth (*Latimeria*
679 *chalumnae*) and elephant shark (*Callorhinchus milii*). The shaded region denotes the
680 catalytic domain. Diagnostic characters -i.e. amino acids positions that distinguish
681 between SIRT3 and SIRT3.2 gene lineages - are indicated with a rectangle and green
682 colors.

683

684 **Figure 7.** Heatmap representation of within-species relative transcriptional levels of
685 sirtuin paralogs between 7 chosen tissues. Transcription values were calculated
686 independently for each species and normalized over all tissues.

687

688 **Figure 8.** Structural model of elephant shark SIRT3.2 and expression of SIRT3.2-like-
689 3myc in mammalian cells. a Superposition of the ribbon representations of elephant shark
690 SIRT3.2 (green model; amino acids G95 to Q365) and human SIRT3 (magenta model;

691 pdb: 4bvh.1.A; amino acids G121 to G392). Depicted in ellipses are the indicated
692 functional/structural domains of SIRT3 and in dotted lines the binding sites for peptide
693 substrates and NAD+. b The indicated cells were left untreated (Control, lanes 1, 3 and
694 5) or transfected to express SIRT3.2-3myc (lanes 2, 4 and 6), followed by immunoblot
695 analysis with antibody against the c-Myc epitope or antibody against β-ACTIN used as
696 loading control. The position of molecular mass markers is indicated on the left. SIRT3.2-
697 3myc exhibits an electrophoretic mobility corresponding to a protein of 48.3 kDa, which
698 is expected considering the extra amino acids of the three copies of the c-Myc epitope at
699 the C-terminus. c and d H4 cells grown in glass coverslips were transfected to express
700 SIRT3.2-3myc (green channel) and incubated with the mitochondrial probe MitoTracker
701 Orange (red channel in c) or mock incubated (d). Cells were fixed, permeabilized, and
702 double- (c) or triple-labeled (d) with mouse monoclonal antibody against the c-Myc
703 epitope (c and d), rabbit polyclonal antibody against the endoplasmic reticulum protein
704 Cytoskeleton-associated protein 4 (P63; d) and sheep polyclonal antibody against the
705 Golgi apparatus protein Trans-Golgi network integral membrane protein 2 (TGN46; c and
706 d). Secondary antibodies were Alexa-Fluor-488-conjugated donkey anti-mouse IgG
707 (green channel), Alexa-Fluor-594-conjugated donkey anti-rabbit IgG (red channel), and
708 Alexa-Fluor-647-conjugated donkey anti-sheep IgG (blue channel), and nuclei were
709 stained with the DNA probe DAPI (white channel). Stained cells were examined by
710 fluorescence microscopy. Insets: X3 magnification with yellow arrows indicating
711 colocalization (c) and green and red arrows indicating lack of colocalization (d). Bar, 10
712 μm.
713
714 **Figure 9.** Comparison of deacetylase activity between human SIRT3 and elephant shark
715 **Δ**NT-SIRT3.2. a-f) Results obtained with a fluorometric deacetylation assay of an
716 acetylated substrate peptide. a) Time course of deacetylase activity at the indicated
717 concentration of SIRT3 and concentrations of **Δ**NT-SIRT3.2. b) Temperature dependence
718 of deacetylase activity. c-d) Michaelis-Menten plot and Lineweaver-Burk plot of SIRT3 (c)
719 and **Δ**NT-SIRT3.2 (d) deacetylase activity. e-f) NAD+ dependence and concentration
720 dependent effects of the SIRT3 inhibitors nicotinamide (NAM) and quercetin (QUE) and
721 of the SIRT3 activator resveratrol (REV) on the deacetylase activity of SIRT3 (e) and

722 ΔNT-SIRT3.2 (f). In a-d, graphs depict the mean ± standard deviation (n = 3). In e-f, bars
723 represent the mean ± standard deviation. Statistical analysis was performed using two-
724 tailed unpaired Student's t-test (n = 3; * $p < 0.05$; ** $p < 0.01$; *** $p < 0.001$; ns, not
725 statistically significant).
726
727 **Figure 10.** SIRT3.2-3myc expression causes an increment on ATP cellular content with
728 no difference in ROS levels. (a) ATP levels were measured by a luciferin/luciferase
729 bioluminescence assay in H4 and HeLa cells either left untreated (Control) or transiently
730 expressing SIRT3.2-3myc. (b) ROS content was measured by the intensity fluorescence
731 of the dye CM-H2DCFDA in H4 and HeLa cells either left untreated (Control) or transiently
732 expressing SIRT3.2-3myc. Bars represent the mean ± standard deviation. Statistical
733 analysis was performed using two-tailed unpaired Student's t-test (n = 4; ** $p < 0.01$; ns,
734 not statistically significant).
735
736

737 Acknowledgements

738 This work was supported by the Fondo Nacional de Desarrollo Científico y Tecnológico
739 from Chile (FONDECYT 1210471) and The Millennium Nucleus of Ion Channel-
740 Associated Diseases is a Millennium Nucleus of the Millennium Scientific Initiative,
741 National Agency of Research and Development (ANID, NCN19_168), Ministry of Science,
742 Technology, Knowledge and Innovation, Chile to JCO, Fondo Nacional de Desarrollo
743 Científico y Tecnológico from Chile (FONDECYT 1211481) to GAM, National Science
744 Foundation (EPS-0903787, DBI-1262901 and DEB-1354147) to F.G.H., Financiamiento
745 Basal No. ANID/BASAL/ACE210009 to PVB and No. ANID/BASAL/FB210008 to PVB
746 and CTR, Fondap-Ideal Grant N° 15150003 and ANID-Millennium Science Initiative
747 Program-Center ICM-ANID ICN2021_002 to LV-C, Fondo Nacional de Desarrollo
748 Científico y Tecnológico from Chile (FONDECYT 1180957) to FJM, Vicerrectoría de
749 Investigación, Desarrollo y Creación Artística, Universidad Austral de Chile to JCO, FJM,
750 LVC, GAM. We thank Stefanie Teuber, John Quiroga and Rafael Burgos, Instituto de
751 Farmacología y Morfofisiología, Facultad de Ciencias Veterinarias, Universidad Austral
752 de Chile, for providing assistance in the use of the Varioskan Flash microplate reader;

Hianara Bustamante, Instituto de Microbiología Clínica, Facultad de Medicina, Universidad Austral de Chile, for providing quercetin and resveratrol; Víctor Castro, Departamento de Biología, Facultad de Ciencias, Universidad de Chile, for providing NAD^+ and nicotinamide; and Gonzalo Astroza, and Andrés Rivera-Dictter for technical assistance.

Contributions

JCO and GAM designed the study. JCO, MWV, FGH, KZ, CM, CL, VC, FJM, PVB, CTR, GAM, collected and/or analyzed data. JCO, PVB and GAM wrote the manuscript. JCO, MWV, FGH, KZ, CM, CL, VC, LV-C, FJM, PVB, CTR and GAM, reviewed and edited the manuscript. All authors contributed to the article and approved the submitted version.

Ethics declarations

Conflict of interest disclosure

The authors declare they have no conflict of interest relating to the content of this article.

Data availability

Data and supplementary material are available online at zenodo.org

References

Albalat R, Cañestro C. 2016. Evolution by gene loss. *Nat. Rev. Genet.* 17:379–391.

Albertson RC, Craig Albertson R, Cresko W, William Detrich H, Postlethwait JH. 2009. Evolutionary mutant models for human disease. *Trends in Genetics* [Internet] 25:74–81. Available from: http://dx.doi.org/10.1016/j.tig.2008.11.006

Altenhoff AM, Train C-M, Gilbert KJ, Mediratta I, Mendes de Farias T, Moi D, Nevers Y, Radoykova H-S, Rossier V, Warwick Vesztrocy A, et al. 2021. OMA orthology in 2021: website overhaul, conserved isoforms, ancestral gene order and more. *Nucleic Acids Res.* 49:D373–D379.

Altschul SF, Gish W, Miller W, Myers EW, Lipman DJ. 1990. Basic local alignment search tool. *J. Mol. Biol.* 215:403–410.

Anderson KA, Green MF, Huynh FK, Wagner GR, Hirschey MD. 2014. SnapShot: Mammalian Sirtuins. *Cell* 159:956–956.e1.

Anders S, Huber W. 2010. Differential expression analysis for sequence count data. *Genome Biol.* 11:R106.

Anisimova M, Gil M, Dufayard J-F, Dessimoz C, Gascuel O. 2011. Survey of branch support methods demonstrates accuracy, power, and robustness of fast likelihood-based approximation schemes. *Syst. Biol.* 60:685–699.

Bause AS, Haigis MC. 2013. SIRT3 regulation of mitochondrial oxidative stress. *Exp. Gerontol.* 48:634–639.

Bilyk KT, Zhuang X, Vargas-Chacoff L, Cheng C-HC. 2021. Evolution of chaperome gene expression and regulatory elements in the antarctic notothenioid fishes. *Heredity* 126:424–441.

Blander G, Guarente L. 2004. The Sir2 family of protein deacetylases. *Annu. Rev. Biochem.* 73:417–435.

Bolger AM, Lohse M, Usadel B. 2014. Trimmomatic: a flexible trimmer for Illumina sequence data. *Bioinformatics* 30:2114–2120.

Bolte S, Cordelières FP. 2006. A guided tour into subcellular colocalization analysis in light microscopy. *J. Microsc.* 224:213–232.

Brown K, Xie S, Qiu X, Mohrin M, Shin J, Liu Y, Zhang D, Scadden DT, Chen D. 2013. SIRT3 reverses aging-associated degeneration. *Cell Rep.* 3:319–327.

Bustamante HA, Cereceda K, González AE, Valenzuela GE, Cheuquemilla Y, Hernández S, Arias-Muñoz E, Cerda-Troncoso C, Bandau S, Soza A, et al. 2020. The Proteasomal Deubiquitinating Enzyme PSMD14 Regulates Macroautophagy

810 by Controlling Golgi-to-ER Retrograde Transport. *Cells* [Internet] 9. Available from:
811 http://dx.doi.org/10.3390/cells9030777

812 Castro LFC, Lopes-Marques M, Gonçalves O, Wilson JM. 2012. The evolution of
813 pepsinogen C genes in vertebrates: duplication, loss and functional diversification.
814 *PLoS One* 7:e32852.

815 Céspedes HA, Zavala K, Vandewege MW, Opazo JC. 2017. Evolution of the α-
816 adrenoreceptors in vertebrates: ADRA2D is absent in mammals and crocodiles.
817 *Gen. Comp. Endocrinol.* 250:85–94.

818 Costantini S, Sharma A, Raucci R, Costantini M, Autiero I, Colonna G. 2013. Genealogy
819 of an ancient protein family: the Sirtuins, a family of disordered members. *BMC*
820 *Evol. Biol.* 13:60.

821 Delsuc F, Brinkmann H, Chourrout D, Philippe H. 2006. Tunicates and not
822 cephalochordates are the closest living relatives of vertebrates. *Nature* 439:965–
823 968.

824 Delsuc F, Tsagkogeorga G, Lartillot N, Philippe H. 2008. Additional molecular support
825 for the new chordate phylogeny. *Genesis* 46:592–604.

826 Di Emidio G, Falone S, Artini PG, Amicarelli F, D'Alessandro AM, Tatone C. 2021.
827 Mitochondrial Sirtuins in Reproduction. *Antioxidants (Basel)* [Internet] 10. Available
828 from: http://dx.doi.org/10.3390/antiox10071047

829 Félix M-A, Barkoulas M. 2015. Pervasive robustness in biological systems. *Nat. Rev.*
830 *Genet.* 16:483–496.

831 Frye RA. 2000. Phylogenetic classification of prokaryotic and eukaryotic Sir2-like
832 proteins. *Biochem. Biophys. Res. Commun.* 273:793–798.

833 Frye RA. 2006. Evolution of Sirtuins From Archaea to Vertebrates. *Histone*
834 *Deacetylases* [Internet]:183–202. Available from: http://dx.doi.org/10.1385/1-59745-
835 024-3:183

836 Fujita Y, Yamashita T. 2018. Sirtuins in Neuroendocrine Regulation and Neurological
837 Diseases. *Front. Neurosci.* 12:778.

838 Gitelman I. 2007. Evolution of the vertebrate twist family and synfunctionalization: a
839 mechanism for differential gene loss through merging of expression domains. *Mol.*
840 *Biol. Evol.* 24:1912–1925.

841 Glover N, Dessimoz C, Ebersberger I, Forslund SK, Gabaldón T, Huerta-Cepas J,
842 Martin M-J, Muffato M, Patricio M, Pereira C, et al. 2019. Advances and
843 Applications in the Quest for Orthologs. *Mol. Biol. Evol.* 36:2157–2164.

844 Glozak MA, Sengupta N, Zhang X, Seto E. 2005. Acetylation and deacetylation of non-

845 histone proteins. *Gene* 363:15–23.

846 Gold DA, Sinclair DA. 2022. Sirtuin Evolution the dawn of animal life. *Mol. Biol. Evol*.
847 39:192.

848 Goldberg T, Hecht M, Hamp T, Karl T, Yachdav G, Ahmed N, Altermann U, Angerer P,
849 Ansorge S, Balasz K, et al. 2014. LocTree3 prediction of localization. *Nucleic Acids*
850 *Res.* 42:W350–W355.

851 Greiss S, Gartner A. 2009. Sirtuin/Sir2 phylogeny, evolutionary considerations and
852 structural conservation. *Mol. Cells* 28:407–415.

853 Haigis MC, Mostoslavsky R, Haigis KM, Fahie K, Christodoulou DC, Murphy AJ,
854 Valenzuela DM, Yancopoulos GD, Karow M, Blander G, et al. 2006. SIRT4 inhibits
855 glutamate dehydrogenase and opposes the effects of calorie restriction in
856 pancreatic beta cells. *Cell* 126:941–954.

857 Haigis MC, Sinclair DA. 2010. Mammalian sirtuins: biological insights and disease
858 relevance. *Annu. Rev. Pathol.* 5:253–295.

859 Hara Y, Yamaguchi K, Onimaru K, Kadota M, Koyanagi M, Keeley SD, Tatsumi K,
860 Tanaka K, Motone F, Kageyama Y, et al. 2018. Shark genomes provide insights
861 into elasmobranch evolution and the origin of vertebrates. *Nat Ecol Evol* 2:1761–
862 1771.

863 Helsen J, Voordeckers K, Vanderwaeren L, Santermans T, Tsontaki M, Verstrepen KJ,
864 Jelier R. 2020. Gene Loss Predictably Drives Evolutionary Adaptation. *Mol. Biol.*
865 *Evol.* 37:2989–3002.

866 Herrero J, Muffato M, Beal K, Fitzgerald S, Gordon L, Pignatelli M, Vilella AJ, Searle
867 SMJ, Amode R, Brent S, et al. 2016. Ensembl comparative genomics resources.
868 *Database* [Internet] 2016. Available from:
869 http://dx.doi.org/10.1093/database/bav096

870 Himmel NJ, Gray TR, Cox DN. 2020. Phylogenetics Identifies Two Eumetazoan TRPM
871 Clades and an Eighth TRP Family, TRP Soromelastatin (TRPS). *Mol. Biol. Evol.*
872 37:2034–2044.

873 Hirschey MD. 2011. Old enzymes, new tricks: sirtuins are NAD(+)-dependent de-
874 acylases. *Cell Metab.* 14:718–719.

875 Hirschey MD, Shimazu T, Goetzman E, Jing E, Schwer B, Lombard DB, Grueter CA,
876 Harris C, Biddinger S, Ilkayeva OR, et al. 2010. SIRT3 regulates mitochondrial
877 fatty-acid oxidation by reversible enzyme deacetylation. *Nature* 464:121–125.

878 Hoang DT, Chernomor O, von Haeseler A, Minh BQ, Vinh LS. 2018. UFBoot2:
879 Improving the Ultrafast Bootstrap Approximation. *Mol. Biol. Evol.* 35:518–522.

880 Howe KL, Achuthan P, Allen J, Allen J, Alvarez-Jarreta J, Amode MR, Armean IM, Azov
881 AG, Bennett R, Bhai J, et al. 2021. Ensembl 2021. *Nucleic Acids Res.* 49:D884–
882 D891.

883 Iwabe N, Hara Y, Kumazawa Y, Shibamoto K, Saito Y, Miyata T, Katoh K. 2005. Sister
884 group relationship of turtles to the bird-crocodilian clade revealed by nuclear DNA-
885 coded proteins. *Mol. Biol. Evol.* 22:810–813.

886 Jara C, Aránguiz A, Cerpa W, Tapia-Rojas C, Quintanilla RA. 2018. Genetic ablation of
887 tau improves mitochondrial function and cognitive abilities in the hippocampus.
888 *Redox Biol* 18:279–294.

889 Kabiljo J, Murko C, Pusch O, Zupkovitz G. 2019. Spatio-temporal expression profile of
890 sirtuins during aging of the annual fish Nothobranchius furzeri. *Gene Expression*
891 *Patterns* [Internet] 33:11–19. Available from:
892 http://dx.doi.org/10.1016/j.gep.2019.05.001

893 Kalyaanamoorthy S, Minh BQ, Wong TKF, von Haeseler A, Jermiin LS. 2017.
894 ModelFinder: fast model selection for accurate phylogenetic estimates. *Nat.*
895 *Methods* 14:587–589.

896 Katoh K, Standley DM. 2013. MAFFT multiple sequence alignment software version 7:
897 improvements in performance and usability. *Mol. Biol. Evol.* 30:772–780.

898 Kumar S, Stecher G, Suleski M, Hedges SB. 2017. TimeTree: A Resource for
899 Timelines, Timetrees, and Divergence Times. *Mol. Biol. Evol.* 34:1812–1819.

900 Kuraku S. 2013. Impact of asymmetric gene repertoire between cyclostomes and
901 gnathostomes. *Semin. Cell Dev. Biol.* 24:119–127.

902 Langmead B, Trapnell C, Pop M, Salzberg SL. 2009. Ultrafast and memory-efficient
903 alignment of short DNA sequences to the human genome. *Genome Biol.* 10:R25.

904 Leinonen R, Sugawara H, Shumway M, International Nucleotide Sequence Database
905 Collaboration. 2011. The sequence read archive. *Nucleic Acids Res.* 39:D19–D21.

906 Li B, Dewey CN. 2011. RSEM: accurate transcript quantification from RNA-Seq data
907 with or without a reference genome. *BMC Bioinformatics* [Internet] 12. Available
908 from: http://dx.doi.org/10.1186/1471-2105-12-323

909 Love MI, Huber W, Anders S. 2014. Moderated estimation of fold change and
910 dispersion for RNA-seq data with DESeq2. *Genome Biol.* 15:550.

911 Lynch M, Conery JS. 2000. The Evolutionary Fate and Consequences of Duplicate
912 Genes. *Science* [Internet] 290:1151–1155. Available from:
913 http://dx.doi.org/10.1126/science.290.5494.1151

914 McBurney MW, Yang X, Jardine K, Hixon M, Boekelheide K, Webb JR, Lansdorp PM,

915 Lemieux M. 2003. The mammalian SIR2alpha protein has a role in embryogenesis
916 and gametogenesis. *Mol. Cell. Biol.* 23:38–54.

917 McCormick SD. 1993. Methods for nonlethal gill biopsy and measurement of Na+, K+-
918 ATPase activity. *Can. J. Fish. Aquat. Sci.* 50:656–658.

919 McDonnell E, Peterson BS, Bomze HM, Hirschey MD. 2015. SIRT3 regulates
920 progression and development of diseases of aging. *Trends Endocrinol. Metab.*
921 26:486–492.

922 Michan S, Sinclair D. 2007. Sirtuins in mammals: insights into their biological function.
923 *Biochem. J* 404:1–13.

924 Michishita E, Park JY, Burneskis JM, Barrett JC, Horikawa I. 2005. Evolutionarily
925 conserved and nonconserved cellular localizations and functions of human SIRT
926 proteins. *Mol. Biol. Cell* 16:4623–4635.

927 Nei M, Rooney AP. 2005. Concerted and birth-and-death evolution of multigene
928 families. *Annu. Rev. Genet.* 39:121–152.

929 Nery MF, Arroyo JI, Opazo JC. 2014. Increased rate of keratin gene loss in the
930 cetacean lineage. *BMC Genomics*. 2014. 15:869.

931 Nguyen NTT, Vincens P, Roest Crollius H, Louis A. 2018. Genomicus 2018: karyotype
932 evolutionary trees and on-the-fly synteny computing. *Nucleic Acids Res.* 46:D816–
933 D822.

934 North BJ, Verdin E. 2004. Sirtuins: Sir2-related NAD-dependent protein deacetylases.
935 *Genome Biol.* 5:224.

936 Ohno S. 1985. Dispensable genes. *Trends Genet.* 1:160–164.

937 Olesen MA, Torres AK, Jara C, Murphy MP, Tapia-Rojas C. 2020. Premature synaptic
938 mitochondrial dysfunction in the hippocampus during aging contributes to memory
939 loss. *Redox Biol* 34:101558.

940 Olson MV. 1999. When less is more: gene loss as an engine of evolutionary change.
941 *Am. J. Hum. Genet.* 64:18–23.

942 Onyango P, Celic I, McCaffery JM, Boeke JD, Feinberg AP. 2002. SIRT3, a human
943 SIR2 homologue, is an NAD-dependent deacetylase localized to mitochondria.
944 *Proc. Natl. Acad. Sci. U. S. A.* 99:13653–13658.

945 Opazo JC, Hoffmann FG, Zavala K, Edwards SV. 2019. Evolution of the DAN gene
946 family in vertebrates. *Evolutionary Biology*:185.

947 Opazo JC, Kuraku S, Zavala K, Toloza-Villalobos J, Hoffmann FG. 2019. Evolution of
948 nodal and nodal-related genes and the putative composition of the heterodimers

949 that trigger the nodal pathway in vertebrates. *Evolution & Development* [Internet]
950 21:205–217. Available from: http://dx.doi.org/10.1111/ede.12292

951 Opazo JC, Vandewege MW, Gutierrez J, Zavala K, Vargas-Chacoff L, Morera FJ,
952 Mardones GA. 2021. Independent duplications of the Golgi phosphoprotein 3
953 oncogene in birds. *Sci. Rep.* 11:12483.

954 Pereira TCB, Rico EP, Rosemberg DB, Schirmer H, Dias RD, Souto AA, Bonan CD,
955 Bogo MR. 2011. Zebrafish as a model organism to evaluate drugs potentially able
956 to modulate sirtuin expression. *Zebrafish* 8:9–16.

957 Ponnambalam S, Girotti M, Yaspo ML, Owen CE, Perry AC, Suganuma T, Nilsson T,
958 Fried M, Banting G, Warren G. 1996. Primate homologues of rat TGN38: primary
959 structure, expression and functional implications. *J. Cell Sci.* 109 (Pt 3):675–685.

960 Qiu H, Hildebrand F, Kuraku S, Meyer A. 2011. Unresolved orthology and peculiar
961 coding sequence properties of lamprey genes: the KCNA gene family as test case.
962 *BMC Genomics* 12:325.

963 Qiu X, Brown K, Hirschey MD, Verdin E, Chen D. 2010. Calorie restriction reduces
964 oxidative stress by SIRT3-mediated SOD2 activation. *Cell Metab.* 12:662–667.

965 Rajabi N, Galleano I, Madsen AS, Olsen CA. 2018. Targeting Sirtuins: Substrate
966 Specificity and Inhibitor Design. *Prog. Mol. Biol. Transl. Sci.* 154:25–69.

967 Ramos-Vicente D, Ji J, Gratacòs-Batlle E, Gou G, Reig-Viader R, Luís J, Burguera D,
968 Navas-Perez E, García-Fernández J, Fuentes-Prior P, et al. 2018. Metazoan
969 evolution of glutamate receptors reveals unreported phylogenetic groups and
970 divergent lineage-specific events. *Elife* [Internet] 7. Available from:
971 http://dx.doi.org/10.7554/eLife.35774

972 Ross BH, Lin Y, Corales EA, Burgos PV, Mardones GA. 2014. Structural and functional
973 characterization of cargo-binding sites on the μ4-subunit of adaptor protein complex
974 4. *PLoS One* 9:e88147.

975 Rueden CT, Schindelin J, Hiner MC, DeZonia BE, Walter AE, Arena ET, Eliceiri KW.
976 2017. ImageJ2: ImageJ for the next generation of scientific image data. *BMC*
977 *Bioinformatics* 18:529.

978 Saravia J, Paschke K, Oyarzún-Salazar R, Cheng C-HC, Navarro JM, Vargas-Chacoff
979 L. 2021. Effects of warming rates on physiological and molecular components of
980 response to CTMax heat stress in the Antarctic fish Harpagifer antarcticus. *J.*
981 *Therm. Biol.* 99:103021.

982 Sauve AA, Schramm VL. 2003. Sir2 regulation by nicotinamide results from switching
983 between base exchange and deacetylation chemistry. *Biochemistry* 42:9249–9256.

984 Scher MB, Vaquero A, Reinberg D. 2007. SirT3 is a nuclear NAD+-dependent histone

985 deacetylase that translocates to the mitochondria upon cellular stress. *Genes Dev.*
986 21:920–928.

987 Schneider CA, Rasband WS, Eliceiri KW. 2012. NIH Image to ImageJ: 25 years of
988 image analysis. *Nat. Methods* 9:671–675.

989 Scholte LLS, Mourão MM, Pais FS-M, Melesina J, Robaa D, Volpini AC, Sippl W, Pierce
990 RJ, Oliveira G, Nahum LA. 2017. Evolutionary relationships among protein lysine
991 deacetylases of parasites causing neglected diseases. *Infect. Genet. Evol.* 53:175–
992 188.

993 Schwartz S, Zhang Z, Frazer KA, Smit A, Riemer C, Bouck J, Gibbs R, Hardison R,
994 Miller W. 2000. PipMaker--a web server for aligning two genomic DNA sequences.
995 *Genome Res.* 10:577–586.

996 Schweizer A, Ericsson M, Bächi T, Griffiths G, Hauri HP. 1993. Characterization of a
997 novel 63 kDa membrane protein. Implications for the organization of the ER-to-
998 Golgi pathway. *J. Cell Sci.* 104 (Pt 3):671–683.

999 Schwer B, North BJ, Frye RA, Ott M, Verdin E. 2002. The human silent information
1000 regulator (Sir)2 homologue hSIRT3 is a mitochondrial nicotinamide adenine
1001 dinucleotide-dependent deacetylase. *J. Cell Biol.* 158:647–657.

1002 Shahgaldi S, Kahmini FR. 2021. A comprehensive review of Sirtuins: With a major focus
1003 on redox homeostasis and metabolism. *Life Sci.* 282:119803.

1004 Sharma S, Ciufo S, Starchenko E, Darji D, Chlumsky L, Karsch-Mizrachi I, Schoch CL.
1005 2019. The NCBI BioCollections Database. *Database* [Internet] 2019. Available
1006 from: http://dx.doi.org/10.1093/database/baz057

1007 Sheffield P, Garrard S, Derewenda Z. 1999. Overcoming expression and purification
1008 problems of RhoGDI using a family of “parallel” expression vectors. *Protein Expr.*
1009 *Purif.* 15:34–39.

1010 Simó-Mirabet P, Bermejo-Nogales A, Calduch-Giner JA, Pérez-Sánchez J. 2017.
1011 Tissue-specific gene expression and fasting regulation of sirtuin family in gilthead
1012 sea bream (Sparus aurata). *Journal of Comparative Physiology B* [Internet]
1013 187:153–163. Available from: http://dx.doi.org/10.1007/s00360-016-1014-0

1014 Slade KM, Freggiaro S, Cottrell KA, Smith JJ, Wiley EA. 2011. Sirtuin-mediated nuclear
1015 differentiation and programmed degradation in Tetrahymena. *BMC Cell Biol.* 12:40.

1016 Smith JJ, Kuraku S, Holt C, Sauka-Spengler T, Jiang N, Campbell MS, Yandell MD,
1017 Manousaki T, Meyer A, Bloom OE, et al. 2013. Sequencing of the sea lamprey
1018 (Petromyzon marinus) genome provides insights into vertebrate evolution. *Nat.*
1019 *Genet.* 45:415–421, 421e1–e2.

1020 Somero GN. 2004. Adaptation of enzymes to temperature: searching for basic

1021 “strategies.” *Comp. Biochem. Physiol. B Biochem. Mol. Biol.* 139:321–333.

1022 Stelzer G, Rosen N, Plaschkes I, Zimmerman S, Twik M, Fishilevich S, Stein TI, Nudel
1023 R, Lieder I, Mazor Y, et al. 2016. The GeneCards Suite: From Gene Data Mining to
1024 Disease Genome Sequence Analyses. *Curr. Protoc. Bioinformatics* 54:1.30.1–
1025 1.30.33.

1026 Tao R, Coleman MC, Pennington JD, Ozden O, Park S-H, Jiang H, Kim H-S, Flynn CR,
1027 Hill S, Hayes McDonald W, et al. 2010. Sirt3-mediated deacetylation of
1028 evolutionarily conserved lysine 122 regulates MnSOD activity in response to stress.
1029 *Mol. Cell* 40:893–904.

1030 Tatone C, Di Emidio G, Barbonetti A, Carta G, Luciano AM, Falone S, Amicarelli F.
1031 2018. Sirtuins in gamete biology and reproductive physiology: emerging roles and
1032 therapeutic potential in female and male infertility. *Hum. Reprod. Update* 24:267–
1033 289.

1034 Tenorio MJ, Ross BH, Luchsinger C, Rivera-Dictter A, Arriagada C, Acuña D, Aguilar M,
1035 Cavieres V, Burgos PV, Ehrenfeld P, et al. 2016. Distinct Biochemical Pools of
1036 Golgi Phosphoprotein 3 in the Human Breast Cancer Cell Lines MCF7 and MDA-
1037 MB-231. *PLoS One* 11:e0154719.

1038 Trifinopoulos J, Nguyen L-T, von Haeseler A, Minh BQ. 2016. W-IQ-TREE: a fast online
1039 phylogenetic tool for maximum likelihood analysis. *Nucleic Acids Res.* 44:W232–
1040 W235.

1041 Tseng AHH, Shieh S-S, Wang DL. 2013. SIRT3 deacetylates FOXO3 to protect
1042 mitochondria against oxidative damage. *Free Radic. Biol. Med.* 63:222–234.

1043 Vassilopoulos A, Fritz KS, Petersen DR, Gius D. 2011. The human sirtuin family:
1044 evolutionary divergences and functions. *Hum. Genomics* 5:485–496.

1045 Vassilopoulos A, Pennington JD, Andresson T, Rees DM, Bosley AD, Fearnley IM, Ham
1046 A, Flynn CR, Hill S, Rose KL, et al. 2014. SIRT3 deacetylates ATP synthase F1
1047 complex proteins in response to nutrient- and exercise-induced stress. *Antioxid.*
1048 *Redox Signal.* 21:551–564.

1049 Vazquez BN, Vaquero A, Schindler K. 2020. Sirtuins in female meiosis and in
1050 reproductive longevity. *Mol. Reprod. Dev.* 87:1175–1187.

1051 Waterhouse A, Bertoni M, Bienert S, Studer G, Tauriello G, Gumienny R, Heer FT, de
1052 Beer TAP, Rempfer C, Bordoli L, et al. 2018. SWISS-MODEL: homology modelling
1053 of protein structures and complexes. *Nucleic Acids Res.* 46:W296–W303.

1054 Wichmann IA, Zavala K, Hoffmann FG, Vandewege MW, Corvalán AH, Amigo JD,
1055 Owen GI, Opazo JC. 2016. Evolutionary history of the reprimo tumor suppressor
1056 gene family in vertebrates with a description of a new reprimo gene lineage. *Gene*
1057 591:245–254.

1058 Wood JG, Rogina B, Lavu S, Howitz K, Helfand SL, Tatar M, Sinclair D. 2004. Sirtuin
1059 activators mimic caloric restriction and delay ageing in metazoans. *Nature*
1060 430:686–689.

1061 Yang L, Ma X, He Y, Yuan C, Chen Q, Li G, Chen X. 2017. Sirtuin 5: a review of
1062 structure, known inhibitors and clues for developing new inhibitors. *Sci. China Life*
1063 *Sci.* 60:249–256.

1064 Yates AD, Achuthan P, Akanni W, Allen J, Allen J, Alvarez-Jarreta J, Amode MR,
1065 Armean IM, Azov AG, Bennett R, et al. 2020. Ensembl 2020. *Nucleic Acids Res.*
1066 48:D682–D688.

1067 You W, Zheng W, Weiss S, Chua KF, Steegborn C. 2019. Structural basis for the
1068 activation and inhibition of Sirtuin 6 by quercetin and its derivatives. *Sci. Rep.*
1069 9:19176.

1070 Zhang J, Xiang H, Liu J, Chen Y, He R-R, Liu B. 2020. Mitochondrial Sirtuin 3: New
1071 emerging biological function and therapeutic target. *Theranostics* 10:8315–8342.

1072 Zhao E, Hou J, Ke X, Abbas MN, Kausar S, Zhang L, Cui H. 2019. The Roles of Sirtuin
1073 Family Proteins in Cancer Progression. *Cancers* [Internet] 11. Available from:
1074 http://dx.doi.org/10.3390/cancers11121949

1075 Zhao H-C, Ding T, Ren Y, Li T-J, Li R, Fan Y, Yan J, Zhao Y, Li M, Yu Y, et al. 2016.
1076 Role of Sirt3 in mitochondrial biogenesis and developmental competence of human
1077 in vitro matured oocytes. *Hum. Reprod.* 31:607–622.

Figure 1

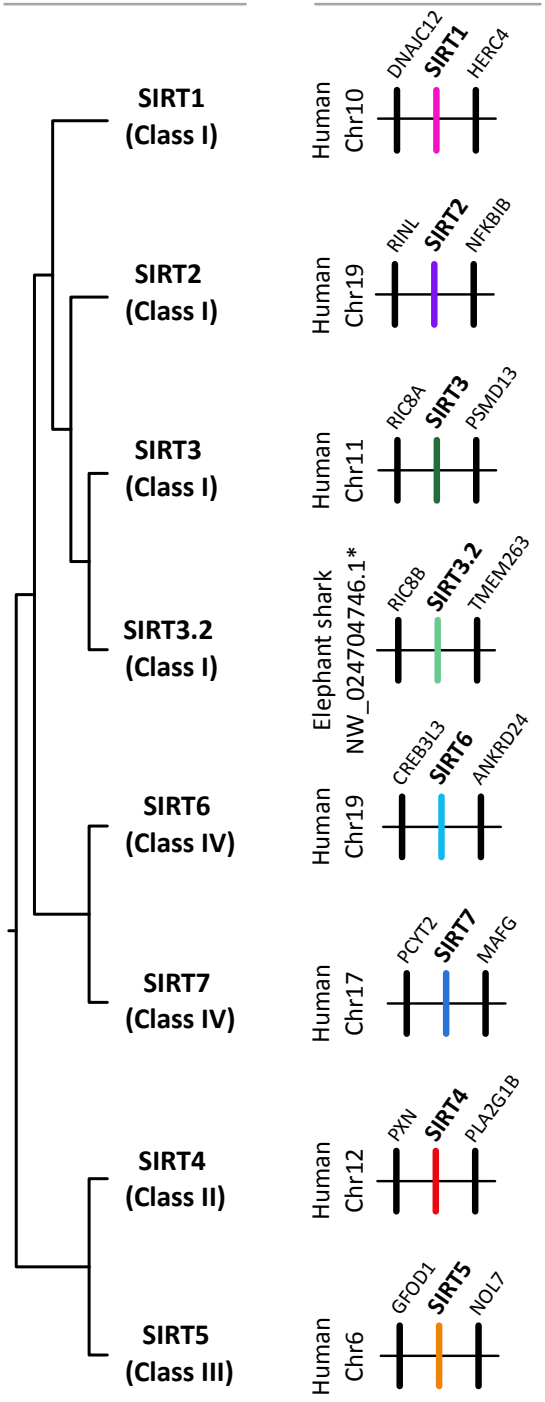

Gene phylogeny	Synteny	Protein Size (AA)	MW (KD)	Enzymatic activity	Subcellular localization	Function	Disease
SIRT1 (Class I)	Human Chr10	747	81.7	Deacetylase	Nucleus & Cytosol	Metabolism regulation, Regulation of chromatin and transcription, DNA repair & Inflammation suppression	Aging, Neurodegenration, Metabolic disease, Cardiovascular disease & Cancer
SIRT2 (Class I)	Human Chr19	389	41.5	Deacetylase	Nucleus & Cytosol	Cell differentiation, Metabolism regulation, Cell cycle regulation, Microtubule dynamics & Inflammation regulation	Cancer & Neurodegeneration
SIRT3 (Class I)	Human Chr11	399	43.6	Deacetylase	Nucleus & Mitochondria	Metabolism regulation, Inflammation suppression, Inhibition of oxidative stress, Apoptosis regulation & Autophagy regulation	Aging, Neurodegenration, Metabolic disease, Cardiovascular disease & Cancer
SIRT3.2 (Class I)	Elephant shark NW_024704746.1*	401	44.2	Deacetylase	Mitochondria	?	?
SIRT6 (Class IV)	Human Chr19	355	39.1	Deacetylase & ADP-ribosyltransferase	Nucleus	Metabolism regulation & Chromatin and DNA repair	Aging, Metabolic disease, Cardiovascular disease & Cancer
SIRT7 (Class IV)	Human Chr17	400	44.9	Deacetylase	Nucleus	Transcription regulation, Chromatin remodeling & Metabolism regulation	Metabolic disease, Cardiovascular disease & Cancer
SIRT4 (Class II)	Human Chr12	314	35.2	ADP-ribosyltransferase, Lipoamidase & Deacetylase	Mitochondria	Metabolism regulation	Neurodegenration, Metabolic disease & Cancer
SIRT5 (Class III)	Human Chr6	310	33.9	Deacetylase, Desuccinylase, Deglutarylase & Demalonylase	Mitochondria	Metabolism regulation & Immune response modulation	Metabolic disease, & Cancer

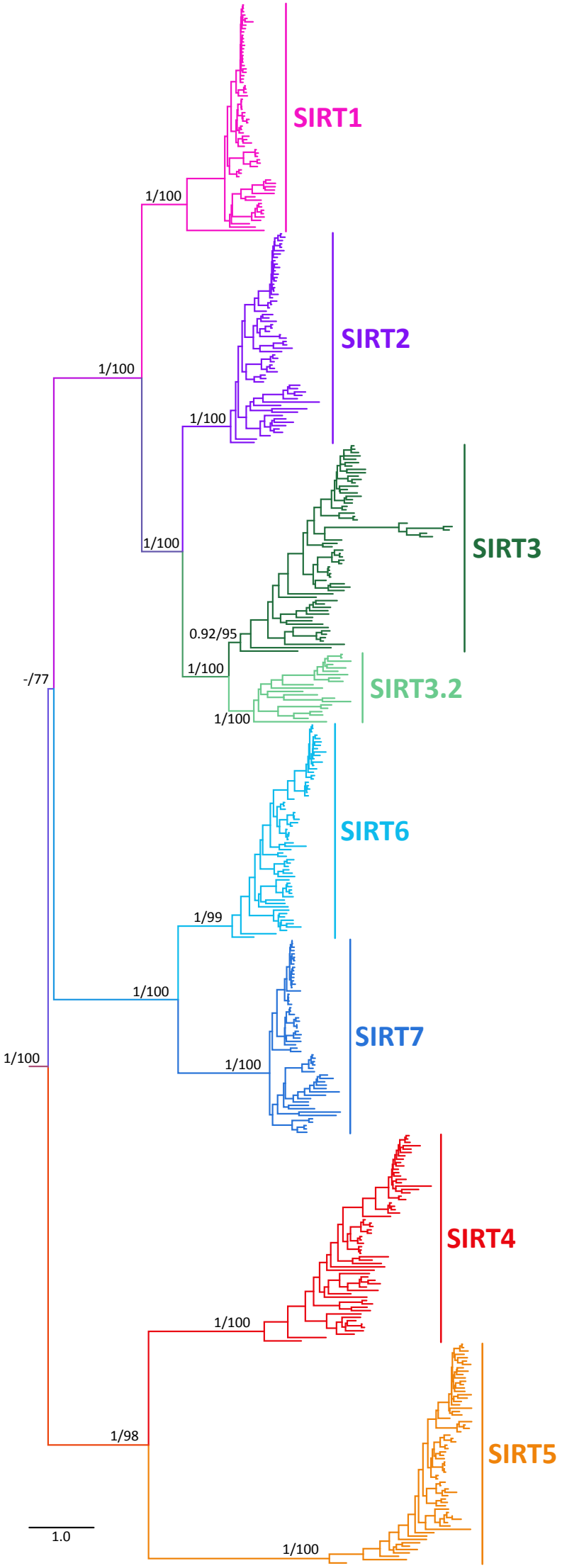
SIRT1
SIRT2
SIRT3
SIRT3.2
SIRT6
SIRT7
SIRT4
SIRT5
1/100
1/100
1/100
1/100
0.92/95
1/100
1/100
-/77
1/99
1/100
1/100
1/100
1/100
1/98
1/100
1.0

Figure 2

Figure 3

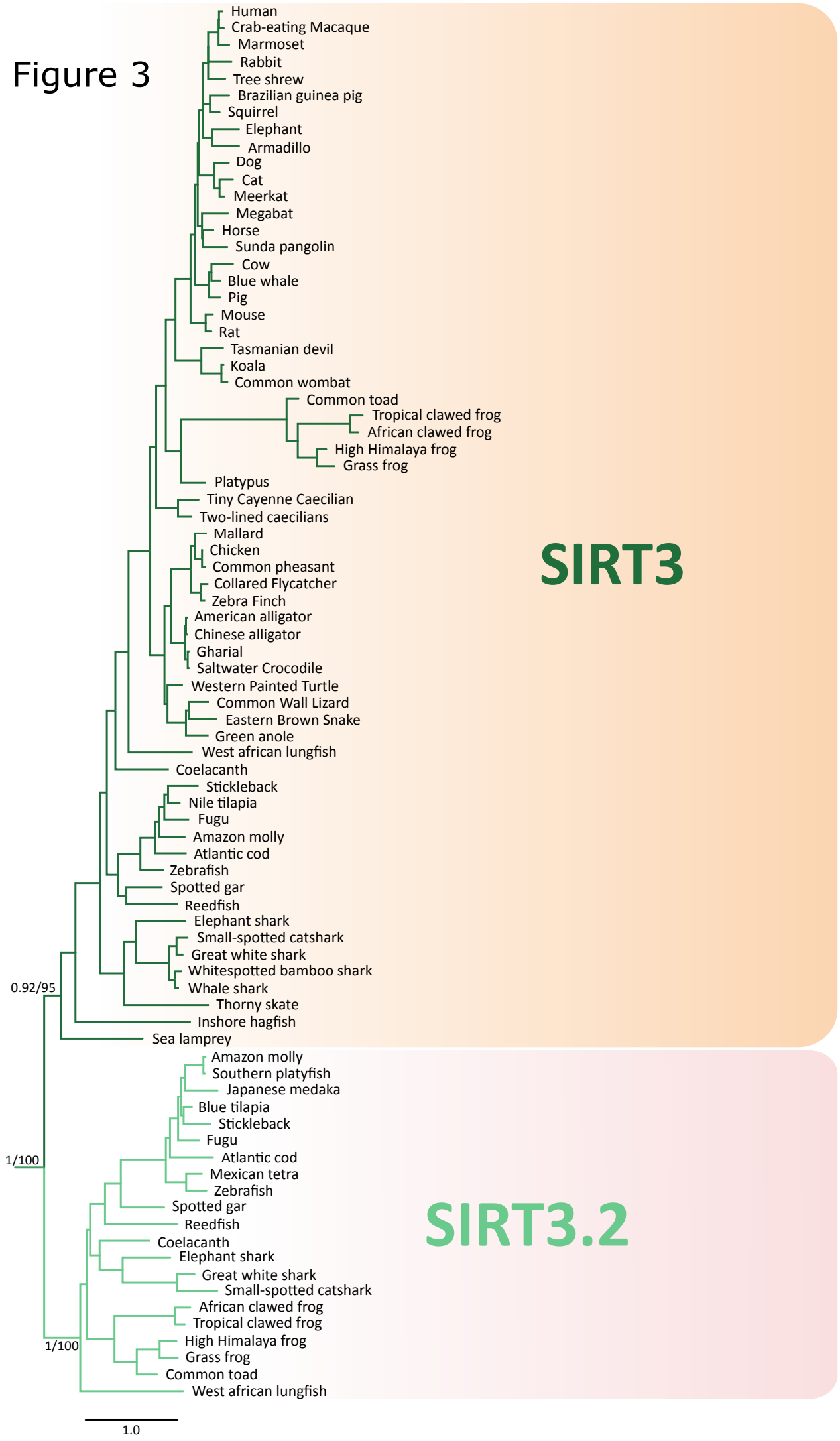
Human
Crab-eating Macaque
Marmoset
Rabbit
Tree shrew
Brazilian guinea pig
Squirrel
Elephant
Armadillo
Dog
Cat
Meerkat
Megabat
Horse
Sunda pangolin
Cow
Blue whale
Pig
Mouse
Rat
Tasmanian devil
Koala
Common wombat
Common toad
Tropical clawed frog
African clawed frog
High Himalaya frog
Grass frog
Platypus
Tiny Cayenne Caecilian
Two-lined caecilians
Mallard
Chicken
Common pheasant
Collared Flycatcher
Zebra Finch
American alligator
Chinese alligator
Gharial
Saltwater Crocodile
Western Painted Turtle
Common Wall Lizard
Eastern Brown Snake
Green anole
West african lungfish
Coelacanth
Stickleback
Nile tilapia
Fugu
Amazon molly
Atlantic cod
Zebrafish
Spotted gar
Reedfish
Elephant shark
Small-spotted catshark
Great white shark
Whitespotted bamboo shark
Whale shark
Thorny skate
Inshore hagfish
Sea lamprey
0.92/95
SIRT3
Amazon molly
Southern platyfish
Japanese medaka
Blue tilapia
Stickleback
Fugu
Atlantic cod
Mexican tetra
Zebrafish
Spotted gar
Reedfish
Coelacanth
Elephant shark
Great white shark
Small-spotted catshark
African clawed frog
Tropical clawed frog
High Himalaya frog
Grass frog
Common toad
West african lungfish
1/100
1/100
SIRT3.2
1.0

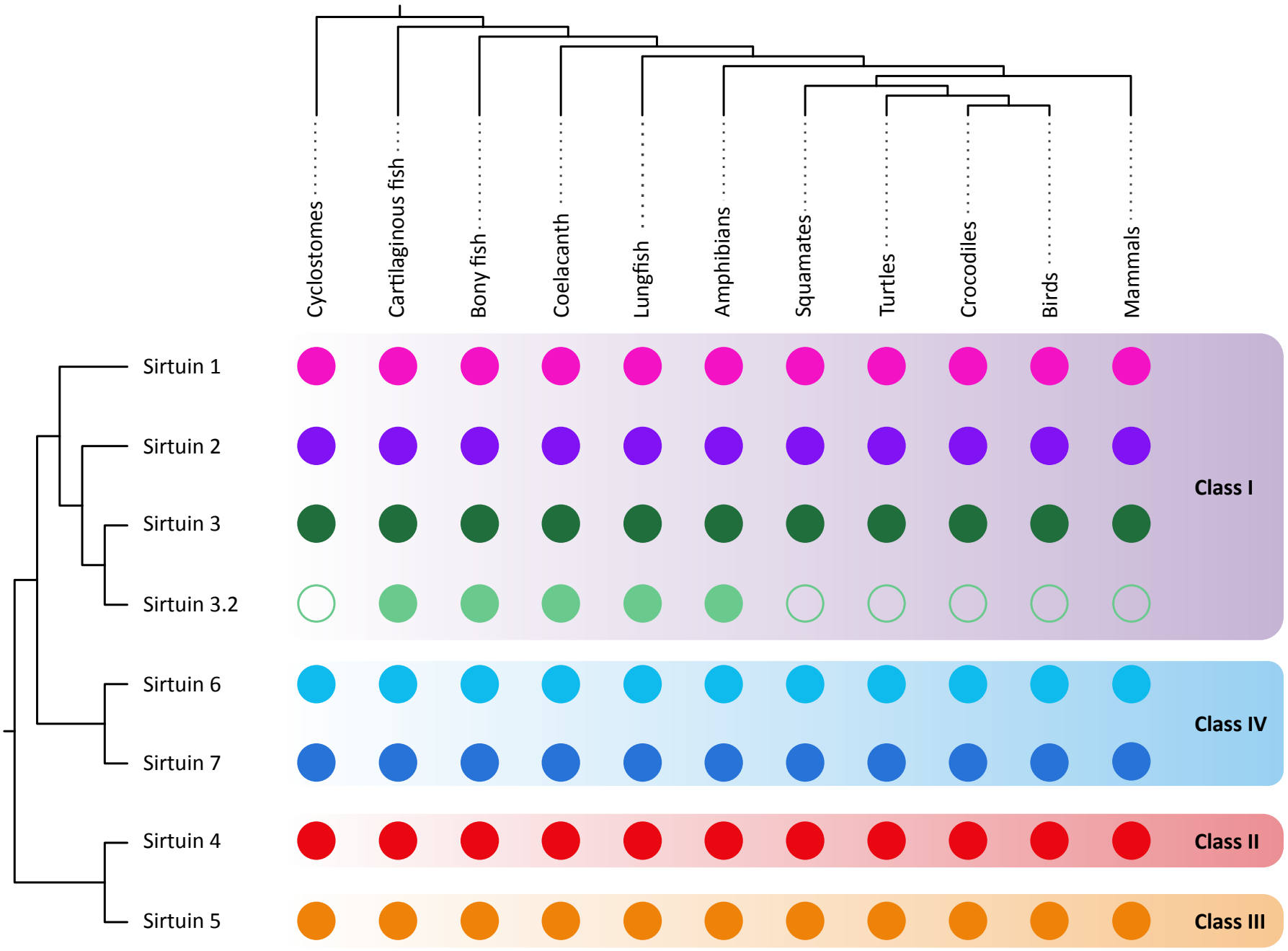
Cyclostomes
Cartilaginous fish
Bony fish
Coelacanth
Lungfish
Amphibians
Squamates
Turtles
Crocodiles
Birds
Mammals
Sirtuin 1
Sirtuin 2
Sirtuin 3
Sirtuin 3.2
Sirtuin 6
Sirtuin 7
Sirtuin 4
Sirtuin 5
Class I
Class IV
Class II
Class III

Figure 4

Figure 5

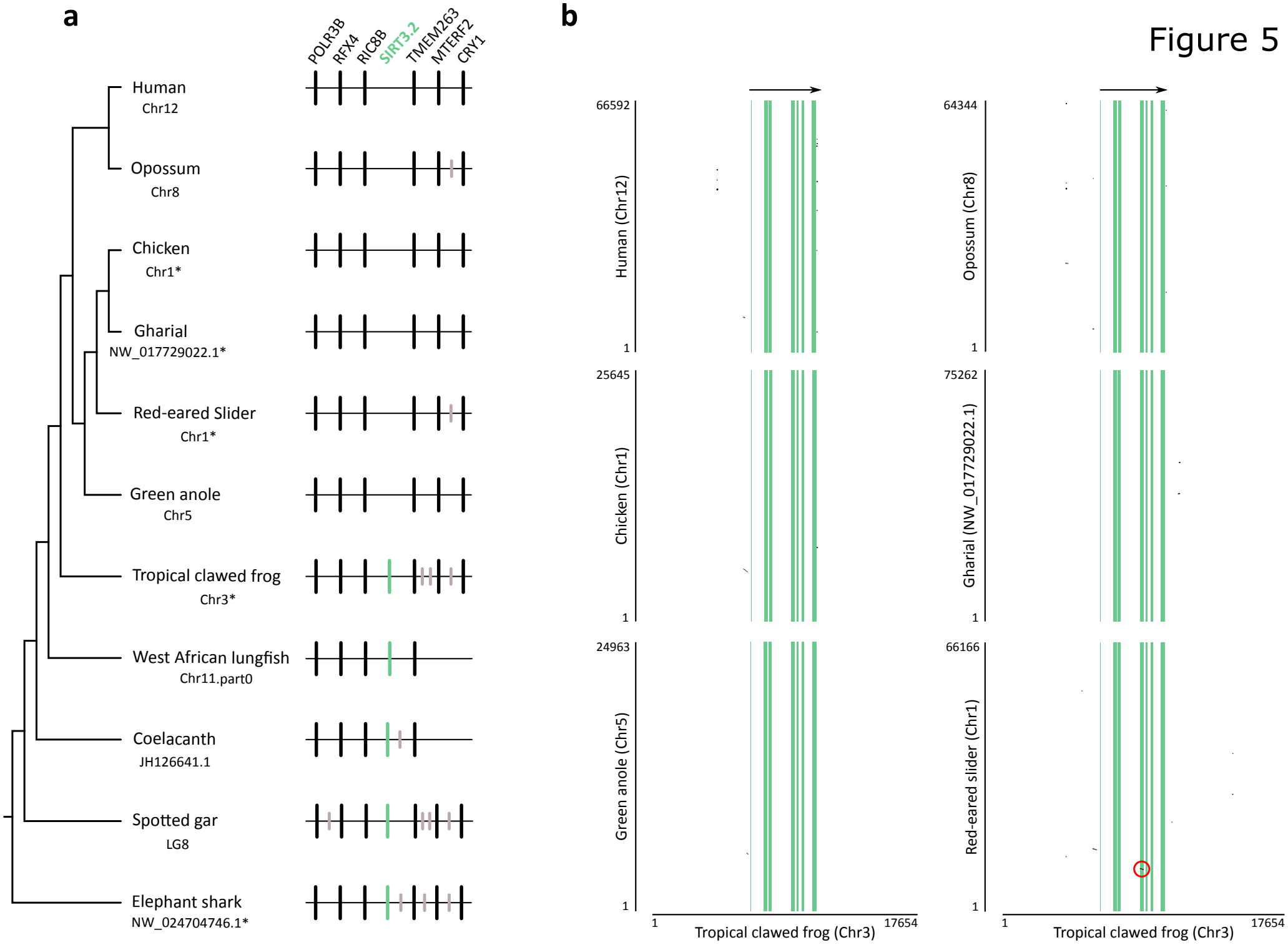
a
POLR3B
RFX4
RIC8B
SIRT3.2
TMEM263
MTERF2
CRY1
Human
Chr12
Opossum
Chr8
Chicken
Chr1*
Gharial
NW_017729022.1*
Red-eared Slider
Chr1*
Green anole
Chr5
Tropical clawed frog
Chr3*
West African lungfish
Chr11.part0
Coelacanth
JH126641.1
Spotted gar
LG8
Elephant shark
NW_024704746.1*
b
66592
Human (Chr12)
1
64344
Opossum (Chr8)
1
25645
Chicken (Chr1)
1
75262
Gharial (NW_017729022.1)
1
24963
Green anole (Chr5)
1
66166
Red-eared slider (Chr1)
1
1
17654
Tropical clawed frog (Chr3)
1
17654
Tropical clawed frog (Chr3)

```
                      116                 126                                                                                                                                                                                                                                                                                                                                                                                                                                                                                                                                                                                                                                                                                                                                                                                                                                                                                                                                                                                                                                                                                                                                                                                                                                                                                                                                                                                                                                                                                                                                                                                                                                                                                                                                                                                                                                                                                                                                                                                                                                                                                                                                                                                                                                                                                                                                                                                                                                                                                                                                                                                                                                                                                                                                                                                                                                                                                                                                                                                                                                                                                                                                                                                                                                                                                                                                                                                                                                                                                                                                                                                                                                                                                                                                                                                                                                                                                                                                                                                                                                                                                                                                                                                                                                                                                                                                                                                                                                                                                                                                                                                                                                                                                                                                                                                                                                                                                                                                                                                                                                                                                                                                                                                                                                                                                                                                                                                                                                                                                                                                                                                                                                                                                                                                                                                                                                                                                                                                                                                                                                                                                                                                                                                                                                                                                                                                                                                                                                                                                                                                                                                                                                                                                                                                                                                                                                                                                                                                                                                                                                                                                                                                                                                                                                                                                                                                                                                                                                                                                                                                                                                                                                                                                                                                                                                                                                                                                                                                                                                                                                                                                                                                                                                                                                                                                                                                                                                                                                                                                                                                                                                                                                                                                                                                                                                                                                                                                                                                                                                                                                                                                                                                                                
Human SIRT3          G S S D K G K L S L Q D V A E L I R A R A C Q R V V V M V G A G I S T P S G I P D F R S P G S G L Y S N L Q Q Y D L P Y P E A I F E L P F F F H N P K P F F T
Coelacanth SIRT3     G G S E Q K Q Q L L E D I A R K I R N R E C N R I V V M A G A G I S T P S G I P D F R S P G S G L Y D N L R H F G I P Y P E A V F E I N Y F L H D P K P F Y S
Spotted gar SIRT3    R G G S Q E Q Q T L Q D V A R F I R D Q E Y K R I V V M A G A G I S T P S G I P D F R S P G S G L Y D N L Q Q Y D L P Y A E A I F E I N Y F R H N P K P F F A
Elephant shark SIRT3 K G S S Q R A S S L E D V A S L V R N K E C Q R I V V M A G A G I S T A S G I P D F R S P G S G L Y D N L Q T Y D I P Y P E A I F E I D Y F H C N P K P F F V
Coelacanth SIRT3.2   P S V G G K L K N L N D I A A L I L Y K R C K N I I I I A G A G I S T A S G I P D F R T P G T G L Y D N L Q Q Y N I P C P E A I F D I D Y F T Y N P K P F F S
Spotted gar SIRT3.2  R R A P S Q L R N L E D V A R L I Q Q R P C R N I I V V A G A G I S T A S G I P D F R T P E S G L Y A N L Q K Y N I P Y P E A I F D I D Y F T C D P Q P F F S
Elephant Shark SIRT3.2 S N A R G K L T K L Q D V A A L I R N R H C R N I V V M A G A G I S T A S G I P D F R T P G T G L Y D N L E E Y N V P Y P E A I F D E S Y F V H N P L P F F S

                      195                                                                                                                                                                                                                                                                                                                                                                                                                                                                                                                                                                                                                                                                                                                                                                                                                                                                                                                                                                                                                                                                                                                                                                                                                                                                                                                                                                                                                                                                                                                                                                                                                                                                                                                                                                                                                                                                                                                                                                                                                                                                                                                                                                                                                                                                                                                                                                                                                                                                                                                                                                                                                                                                                                
Human SIRT3          L A K E L Y P G N Y K P N V T H Y F L R L L H D K G L L L R L Y T Q N I D G L E R V S G I P A S K L V E A H G T F A S A T C T V C Q R P F P G E D I R A D V M
Coelacanth SIRT3     L A K E L Y P G N Y K P N W A H Y F V R L L Y K K G M L L R M Y T Q N I D G L E R L A G I P P S M L V E A H G S F A T A S C T V C C E S Y P G E N F R D E V M
Spotted gar SIRT3    L A K E L Y P G N Y L P N L T H F F I R L L H D K G L L H R M Y T Q N I D G L E R M A G I P S S K L V E A H G T F A T A T C T V C R T S Y P G E A L R A E I L
Elephant shark SIRT3 L A K E L Y P G S C W P N F T H Y F V R L L H Q K G I L L R M Y T Q N I D G L E R M A G I P P E K L V E A H G T F A T A T C T V C L K A Y S W E E L R D D V M
Coelacanth SIRT3.2   L V K E L Y P G N Y Q P N Y I H Y F V K M L H E K G L L L K M Y T Q N I D G L E R K A G I P S E K L V E A H G T F S T A S C H S C C K P F P A K I A Q E A I M
Spotted gar SIRT3.2  L A K E L Y P G C Y R P N Y V H Y F V R M L H E K G L L L R M Y T Q N I D G L E R I S G I P E E K L V E A H G T F S S A S C H L C Y T K F P V T E A K K L I L
Elephant shark SIRT3.2 L A K K L Y T E N Y K P N Y I H Y F L R M L H E K G L L L R L Y T Q N I D G L E R M A G I P S I K M V E A H G T F L T A S C S S C R S P Y P A S K A K A E I L

                      274                                                                                                                                                                                                                                                                                                                                                                                                                                                                                                                                                                                                                                                                                                                                                                                                                                                                                                                                                                                                                                                                                                                                                                                                                                                                                                                                                                                                                                                                                                                                                                                                                                                                                                                                                                                                                                                                                                                                                                                                                                                                                                                                                                                                                                                                                                                                                                                                                                                                                                                                                                                                                                                                                                
Human SIRT3          A D R V P R C P V C T G V V K P D I V F F G E P L P Q R F L - L H V V D F P M A D L L L I L G T S L E V E P F A S L T E A V R S S V P R L L I N R D L V G P L
Coelacanth SIRT3     E G K V P L C P I C T G V I K P D I I F F G Q E L P K R F F - L Y L T D F P L A D L L I I M G T S L E V E P F A S L A G A V R S S V T R L L I N R D L V G P F
Spotted gar SIRT3    E S K I P K C P S C K G V L K P D I V F F G E E L P Q Q F F - L Y L T D F P M A D L L I V M G T S L E V E P F A S L A G A V R S S V P R V L I N R D L V G P F
Elephant shark SIRT3 Q S K V P Q C A T C S G V I K P D I V F F G E Q L P Q K F D - L H M L D L P L A D L L V I M G T S L E V E P F A S L S G M V R G S V P R V L I N Q D L V G S F
Coelacanth SIRT3.2   N D K I P R C K A C S G I V K P D I V F F G E D L P K R F Y - R F S K D F V N A D L V F I M G T S L E I E P F A S I V D S A R S Y V P R L L L N R D L V G P F
Spotted gar SIRT3.2  S N K V P R C K N C Q G T V K P D V V F F G E D L P K K F F - L H T K D F P K A D L L I I M G T S L Q I E P F A S I V N T V K A T V P R L L L N R D P I G P F
Elephant shark SIRT3.2 S D K I P K C K R C T G I V K P D I V F F G E D L P K R F H S L Y R K D F Y K S D L L I V M G T S L E I E P F A G I V N S V Q P N V P R L L L N R D P V G P F

                      352                                                 382                 392
Human SIRT3          A W H P - R S R D V A Q L G D V V H G V E S L V E L L G W T E E M R D L V Q R E T G
Coelacanth SIRT3     S W Y S - R S N D V V E L G E V I G G V R K F V D L L G W K E E M K D L I E R E T E
Spotted gar SIRT3    A Y P S P R P N D V V E Q G D V I T G V Q K F V D T L G W G E E L N E L I A V E T A
Elephant shark SIRT3 V R N P P R G G D V T E L G D I V R G V E R F A E L L G W K Q E V N D L L Q R E H K
Coelacanth SIRT3.2   K R K P M R N T D V A E L G D L I E N I K R L V G I L G W E E K M D E L I R A H T H
Spotted gar SIRT3.2  Q K I P L K R T D F M E L G D L V D G V K M F A R H L G W H E E I E D L I R R H E C
Elephant shark SIRT3.2 Q G K C L K K T D V R A L G D L T K S I Q L F V D M V G W K N D L D E L I Q E R A L
```

Figure 6

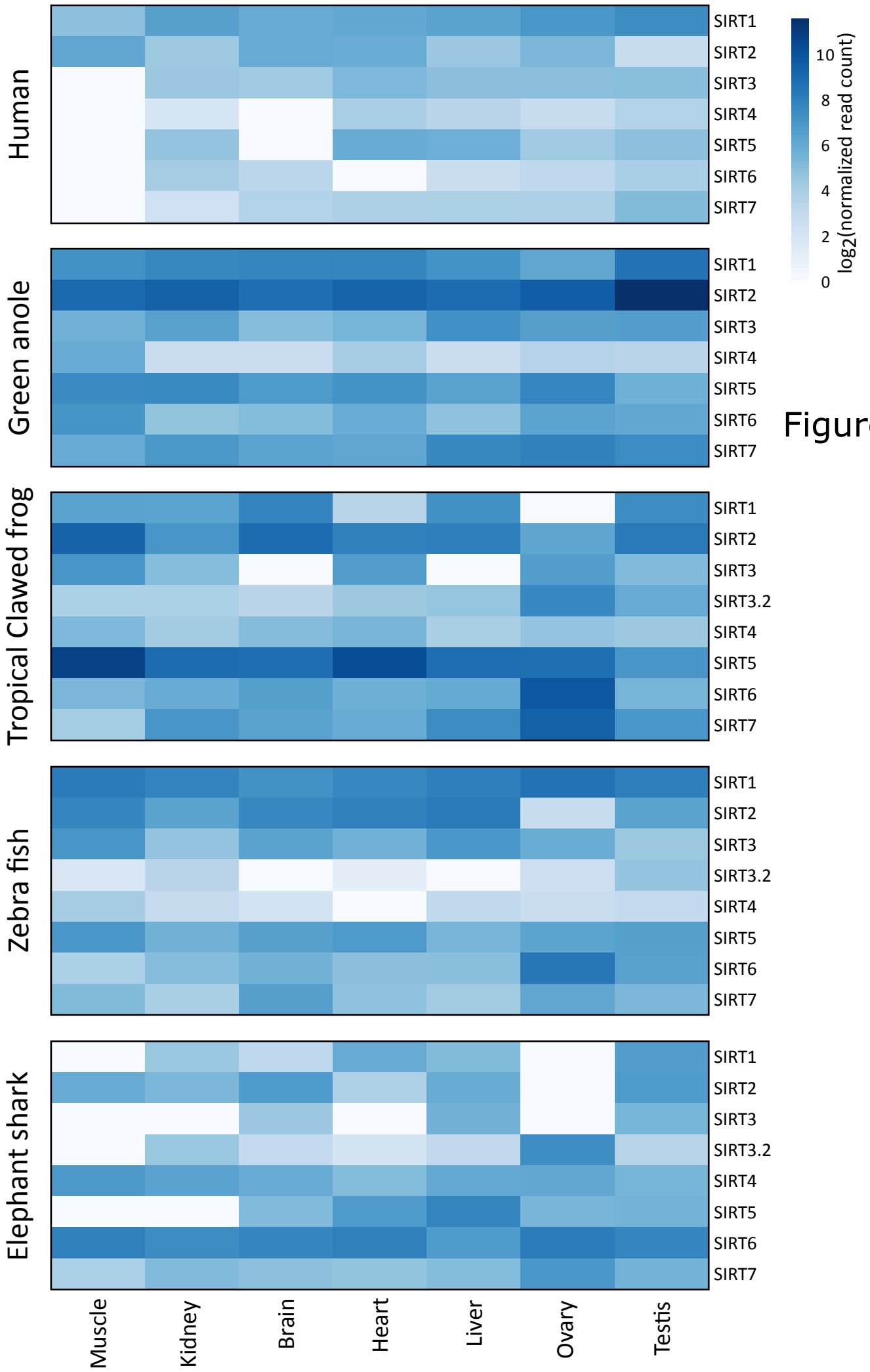
Human
Green anole
Tropical Clawed frog
Zebra fish
Elephant shark
SIRT1
SIRT2
SIRT3
SIRT3.2
SIRT4
SIRT5
SIRT6
SIRT7
Muscle
Kidney
Brain
Heart
Liver
Ovary
Testis
log2(normalized read count)
0
2
4
6
8
10

Figure 7

Figure 8

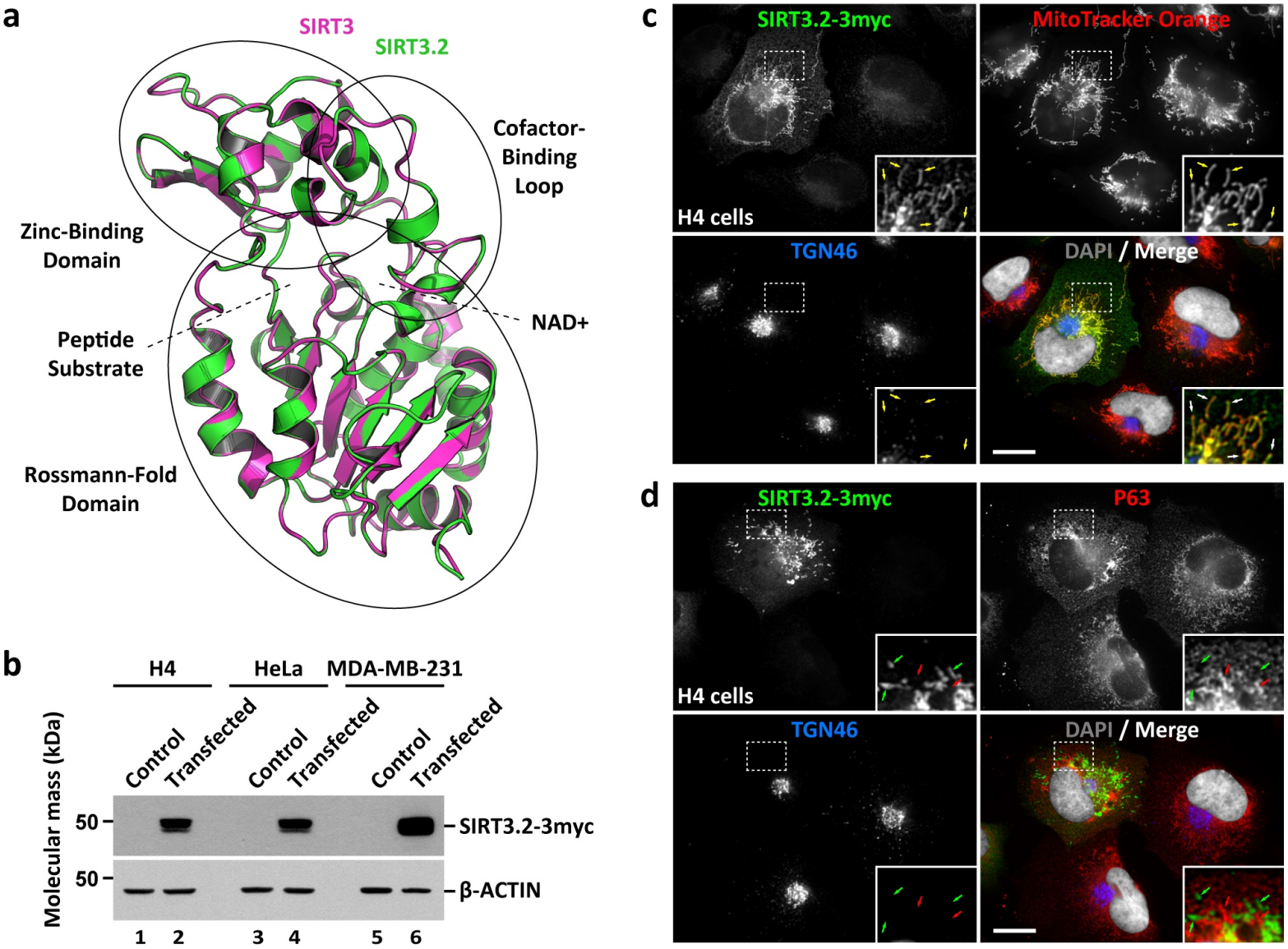
a
SIRT3
SIRT3.2
Cofactor-Binding Loop
Zinc-Binding Domain
NAD+
Peptide Substrate
Rossmann-Fold Domain
b
H4
HeLa
MDA-MB-231
Control
Transfected
Control
Transfected
Control
Transfected
Molecular mass (kDa)
50
50
SIRT3.2-3myc
β-ACTIN
1 2 3 4 5 6
c
SIRT3.2-3myc
MitoTracker Orange
H4 cells
TGN46
DAPI / Merge
d
SIRT3.2-3myc
P63
H4 cells
TGN46
DAPI / Merge

Figure 9

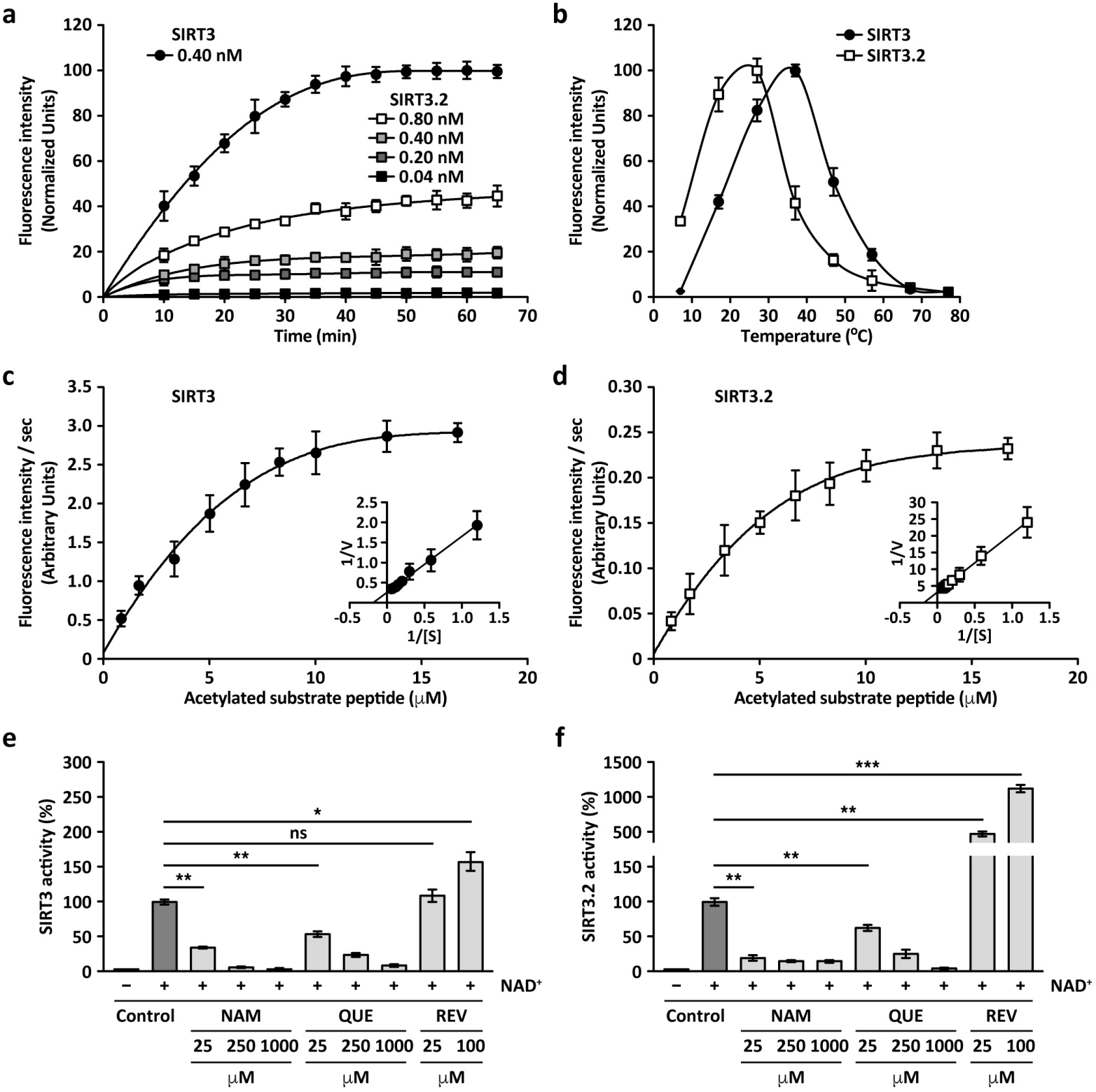
a
SIRT3
0.40 nM
SIRT3.2
0.80 nM
0.40 nM
0.20 nM
0.04 nM
Fluorescence intensity (Normalized Units)
Time (min)
b
SIRT3
SIRT3.2
Fluorescence intensity (Normalized Units)
Temperature (°C)
c
SIRT3
Fluorescence intensity / sec (Arbitrary Units)
Acetylated substrate peptide (μM)
1/V
1/[S]
d
SIRT3.2
Fluorescence intensity / sec (Arbitrary Units)
Acetylated substrate peptide (μM)
1/V
1/[S]
e
SIRT3 activity (%)
*
ns
**
**
NAD+
Control
NAM
QUE
REV
25 250 1000
25 250 1000
25 100
μM
μM
μM
f
SIRT3.2 activity (%)
***
**
**
**
NAD+
Control
NAM
QUE
REV
25 250 1000
25 250 1000
25 100
μM
μM
μM

Figure 10

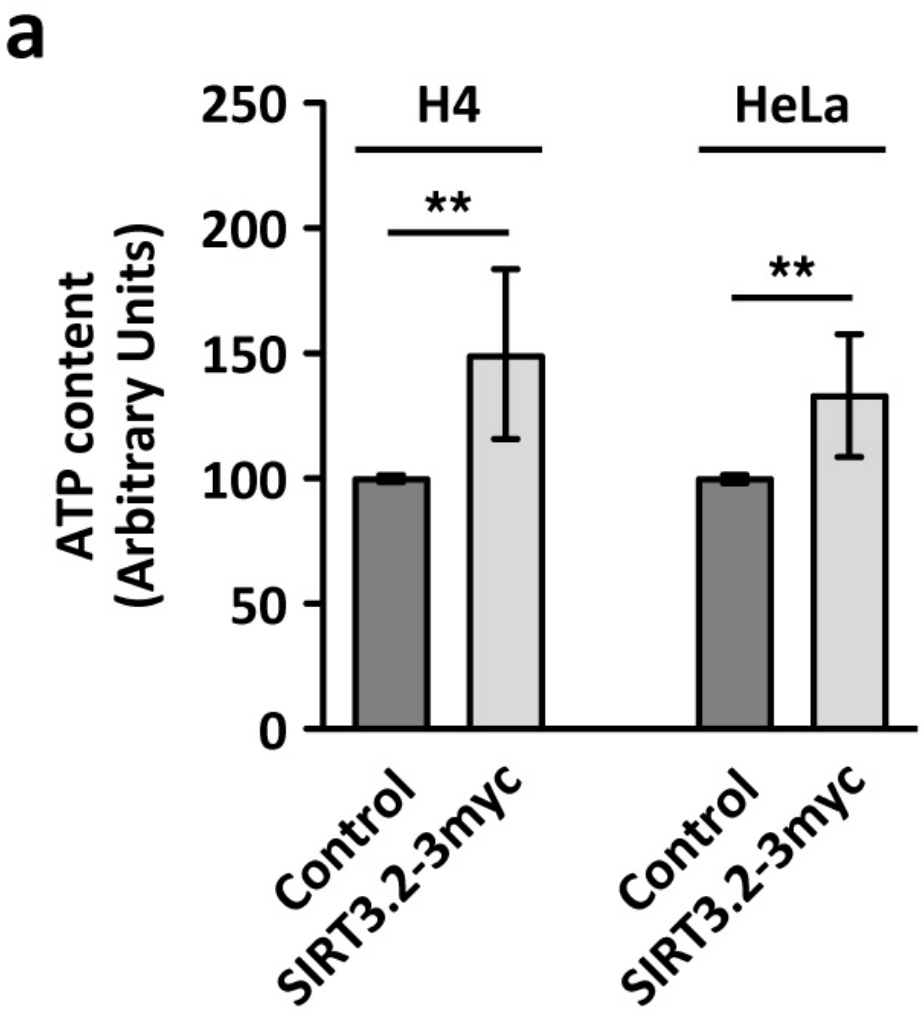
a
250
200
150
100
50
0
ATP content
(Arbitrary Units)
H4
HeLa
**
**
Control
SIRT3.2-3myc
Control
SIRT3.2-3myc

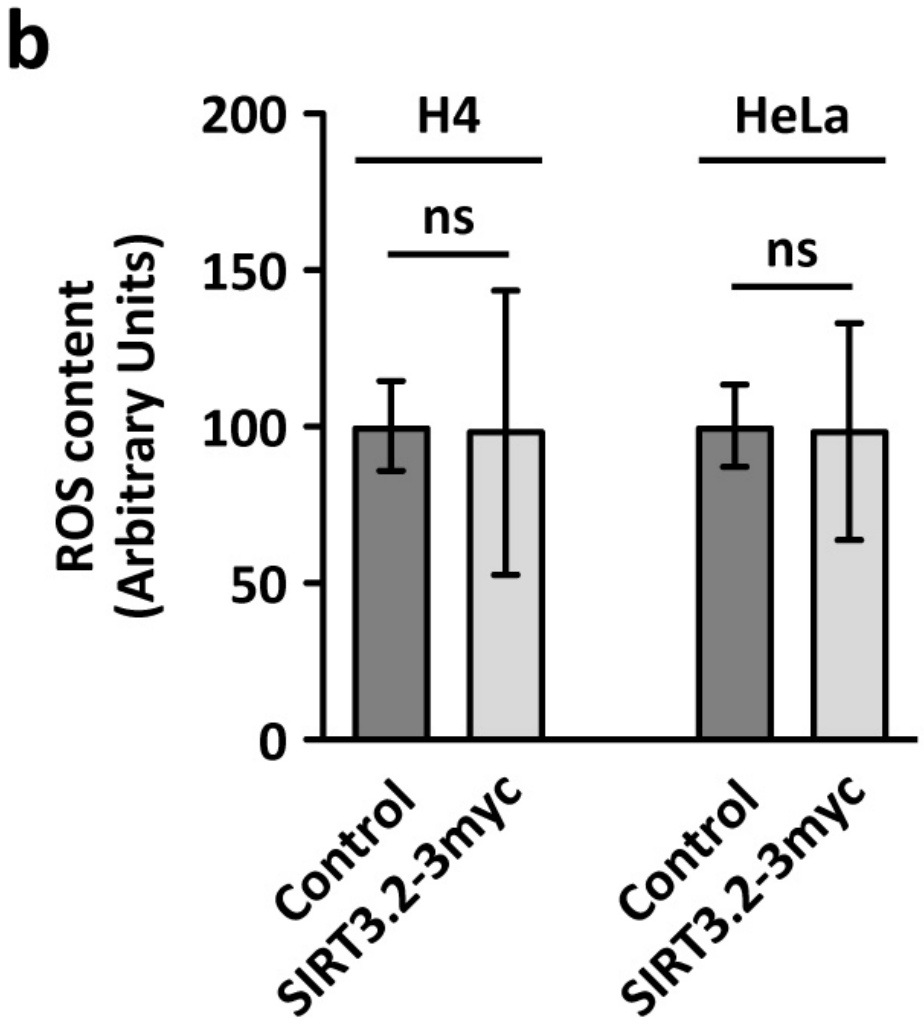
b
200
150
100
50
0
ROS content
(Arbitrary Units)
H4
HeLa
ns
ns
Control
SIRT3.2-3myc
Control
SIRT3.2-3myc